



# Master Thesis

Topic:

Understanding complex bioaccumulation process of inorganic  $\text{Hg}^{2+}$   
from zooplankton by a novel aggregation-induced emission  
fluorogen.

Topic Number and Name:

ENGR9700 Masters Thesis

Semester and Year:

Semester 2 – 2017

Name of Student and ID:

Weixin Ou - 2159707

Supervisor:

Youhong Tang

Co-supervisors:

Jianguang Qin

Tao He

Date of Report Submitted:

11/09/2017

Grade:

College of Science and Engineering

# Declaration

I certify that this work does not incorporate without acknowledgment any material previously submitted for a degree or diploma in any university; and that to the best of my knowledge and belief it does not contain any material previously published or written by another person except where due reference is made in the text.

*Weixin Ou* Weixin Ou

*07/09/2017* 07/09/2017

# Contents

Declaration .....	ii
Abstract.....	v
1. Introduction .....	1
2. Literature Review .....	2
2.1 Bioaccumulation.....	2
2.1.1 Development of tolerance to pollutants.....	2
2.1.2 The problems of biomagnification of pollutants along the trophic level .....	3
2.2 Toxicology of mercury .....	3
2.3 Traditional methods for determining Hg <sup>2+</sup> .....	5
2.3.1 Atomic optical spectroscopy .....	5
2.3.2 Isotopic labeling technique.....	6
2.3.3 Enzymatic inhibition.....	8
2.3.4 Inductively coupled plasma mass spectrometry .....	8
2.4 Novel methodology---- Fluorescent probes.....	9
2.4.1 Aggregation-caused quenching (ACQ) .....	10
2.4.2 Aggregation-induced emission (AIE).....	10
2.5 Methods of Hg <sup>2+</sup> detection using AIEgens .....	12
2.6 Use AIEgens for aquarium system.....	17
2.7 Daphnia.....	22
2.7.1 The status of <i>Daphnia</i> in the trophic level of the aquarium system .....	22
2.7.2 Morphological structure of daphnia .....	23
2.7.3 Mercury toxicity experiment in daphnia.....	23
2.8 Literature review summary .....	24
3. Aim.....	24
4. Materials and Methodology .....	25
4.1. Materials .....	25
4.2 Methodology.....	28

4.2.1 Developing the standard curve of Hg <sup>2+</sup> concentration vs. photoluminescence (PL) intensity ratio using the ratiometric method .....	28
4.2.2 The response to different inorganic Hg <sup>2+</sup> concentration and death rate of <i>Daphnia carinata</i> in the toxic heavy metal solution.....	29
4.2.3 Determine the quantity of Hg <sup>2+</sup> bioaccumulated and bioreleased by <i>Daphnia carinata</i> .....	30
4.2.4 Hg <sup>2+</sup> dynamics in <i>D. carinata</i> by AIEgen visualization in vivo .....	31
4.2.5 The response of <i>Daphnia carinata</i> to inorganic Hg <sup>2+</sup> polluted <i>Euglena gracilis</i> . .....	31
5. Results and Discussion.....	32
5.1 The relationship between PL intensity ratio and Hg <sup>2+</sup> concentration determined by ratiometric method.....	32
5.2 The response of <i>D. carinata</i> to inorganic Hg <sup>2+</sup> and mortality rate estimation. ....	36
5.3 AIEgen quantification for bioaccumulation of inorganic Hg <sup>2+</sup> in <i>D. carinata</i> . ....	39
5.3.1 Absorption of inorganic Hg <sup>2+</sup> in <i>D. carinata</i> . ....	39
5.3.2 Biorelease of inorganic Hg <sup>2+</sup> in <i>D. carinata</i> .....	41
5.3.3 The bioaccumulation of different inorganic Hg <sup>2+</sup> concentrations in <i>D. carinata</i> . ....	43
5.4 In vivo visualization of Hg <sup>2+</sup> dynamics within <i>D. carinata</i> by AIEgen under fluorescence microscope.....	46
5.5 The response of <i>Daphnia carinata</i> to toxic Hg <sup>2+</sup> enriched <i>Euglena gracilis</i> . ....	51
6. Conclusion.....	57
7. Acknowledgements.....	58
8. References.....	58

# Abstract

Aggregation-induced emission fluorogen (AIEgen) was used as a novel material to determine the complicated process of bioaccumulation in a primary consumer (*Daphnia carinata*) in an aquatic microcosm. Inorganic mercury ion ( $\text{Hg}^{2+}$ ) was used as the contaminant. *Daphnia* plays an important role as a primary consumer in the aquatic system, which is essential to develop the understanding of the dynamic of  $\text{Hg}^{2+}$  in bioaccumulation and biorelease in zooplankton. The *Daphnia carinata* was chosen as the experimental organism because it is an essential link to transfer energy from low to high trophic levels. Based on the fluorescence turn-on feature, the specific AIEgen was used to determine the inorganic  $\text{Hg}^{2+}$  concentration in the aquatic system by using the built relationship between the ratio of photoluminescence (PL) intensity at the wavelength of 595/480 nm and  $\text{Hg}^{2+}$  concentrations in the medium. After reaching an equilibrium, the ratio of PL intensity was used to determine the  $\text{Hg}^{2+}$  concentration and then to deduce the quantity of contaminant bioaccumulated by *D. carinata*. The mortality rate of *D. carinata* was recorded at two different  $\text{Hg}^{2+}$  concentrations. The in vivo visualization of  $\text{Hg}^{2+}$  distribution in *D. carinata* revealed the possible cause of *D. carinata* mortality. Besides, the response of *D. carinata* to  $\text{Hg}^{2+}$  via environment absorption was compared with that through food intake of algae *Euglena gracilis* contaminated by  $\text{Hg}^{2+}$ . The *D. carinata* was suffered a much higher mortality by direct  $\text{Hg}^{2+}$  absorption than through food intake. The reason of high mortality after  $\text{Hg}^{2+}$  absorption is possibly due to carapace deformation from the reaction of  $\text{Hg}^{2+}$  with chitin in the carapace but the toxicological pathway leading to death warrants further investigation.

# 1. Introduction

Bioaccumulation is a concept that the toxic substances or pollutants gradually build-up in the living organisms. In the same trophic level, the aquatic organisms accumulate, store and transform the toxic substances or pollutants inside the body. Through this process, the toxic substances in the body would exceed that in the culture medium (Gobas et al. 2009). With the life span becoming longer, the toxic substances are bioaccumulated greater in the body. Moreover, the higher the trophic level is, the greater concentration of the toxic substances absorbed in the body because the organisms in this level are able to consume a large number of organisms at lower trophic levels. Therefore, it can severely affect the growth and development of organisms. The worst consequence of consuming toxic substances is the death of organisms (Kelly et al. 2007). Methyl mercury (MeHg), a toxic heavy metal formed by inorganic  $\text{Hg}^{2+}$ , is easily to accumulate in an organism. The majority amount of human-generated mercury comes from stationary combustion, and one of the largest aggregated source is the coal-fired power plant. The water that is nearby the fuel factory has more chances to get polluted by inorganic  $\text{Hg}^{2+}$ . As a consequence, the toxic  $\text{Hg}^{2+}$  can be bioaccumulated in aquatic organisms. As a result, human beings, the highest level of the food chain, will accumulate the greatest concentration of MeHg. This is going to have an adverse effect on humans' health and endanger humans' lives, which is the most severe situation. Moreover, it becomes a global concern. Therefore, it is essential to find an effective and reasonable way to detect the concentration of  $\text{Hg}^{2+}$ , which is the source of MeHg in the water. MeHg is really harmful to the human's body, and without proper protection, it can cause a long-term negative effect. Therefore, in this thesis, although MeHg can be determined directly, for safety consideration, the

bioaccumulation of MeHg is not included. The only focus point is on inorganic mercury.

## **2. Literature Review**

### **2.1 Bioaccumulation**

Some chemical contaminants can be found ubiquitous in the ocean or freshwater. The organisms in the aquatic system are easily to absorb these toxic substances without excretion (Bryan et al. 1979). The bioaccumulation process occurs based on the aquatic organisms' ability to store the pollutants. When this happens, the concentration of the toxic substances can reach a very high level in an organism, and sometimes the equilibrium level is not able to reach (Bryan et al. 1979).

There are two main aspects that can affect the processes of bioaccumulation, which are the development of tolerance to pollutants and the biomagnification of pollutants along the trophic level (Bryan et al. 1979).

#### **2.1.1 Development of tolerance to pollutants**

After exposure to the toxic substances at a sublethal concentration, the ability of dealing with the toxic substances can be triggered. This causes high possibility of increasing the tolerance of an organism to a pollutant, which means that the organism can have greater capacity to accumulate more toxic substances. Besides, the natural selection also contributes to the bioaccumulation level. After continuing exposure in certain toxic substances, living organisms tend to have higher tolerance for a particular toxicant (Bryan et al. 1979).

### 2.1.2 The problems of biomagnification of pollutants along the trophic level

It is known that the most important way of absorbing the toxic substances usually is from food intake (Bryan et al. 1979). When the lower level organisms have carried certain amount of pollutants and have been eaten by an organism at the high trophic level, those located in the higher level tend to absorb more toxic substance. If those substances are excreted, it is more likely to be accumulated inside the organism. This is because the organisms in the higher trophic level would consume more different species than that in the lower one. Fig 1 shows the process of bioaccumulation in aquatic organisms.

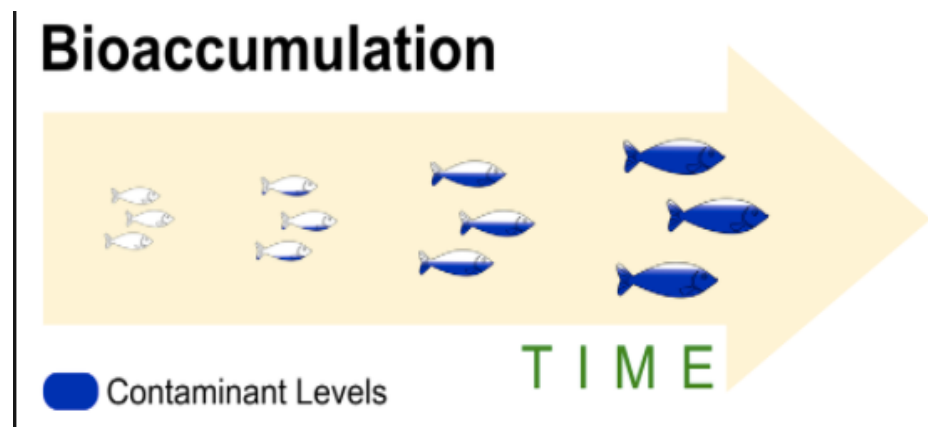


Fig 1. Process of bioaccumulation in aquatic species (Olenick 2013)

## 2.2 Toxicology of mercury

The form of mercury in atmosphere is vaporous mercury (zero valence) because of its low evaporating point at room temperature. The way of  $Hg^{2+}$  oxidation is via the action of ozone. The trace of MeHg is observed in the environment; however, its source is not known. The major transformation from  $Hg^{2+}$  to MeHg in an aquatic organism is caused by bioaccumulation and



the biomagnification in the food chain (Clarkson 1998). Fig 2 shows the current model of the global and chemical cycle of mercury.

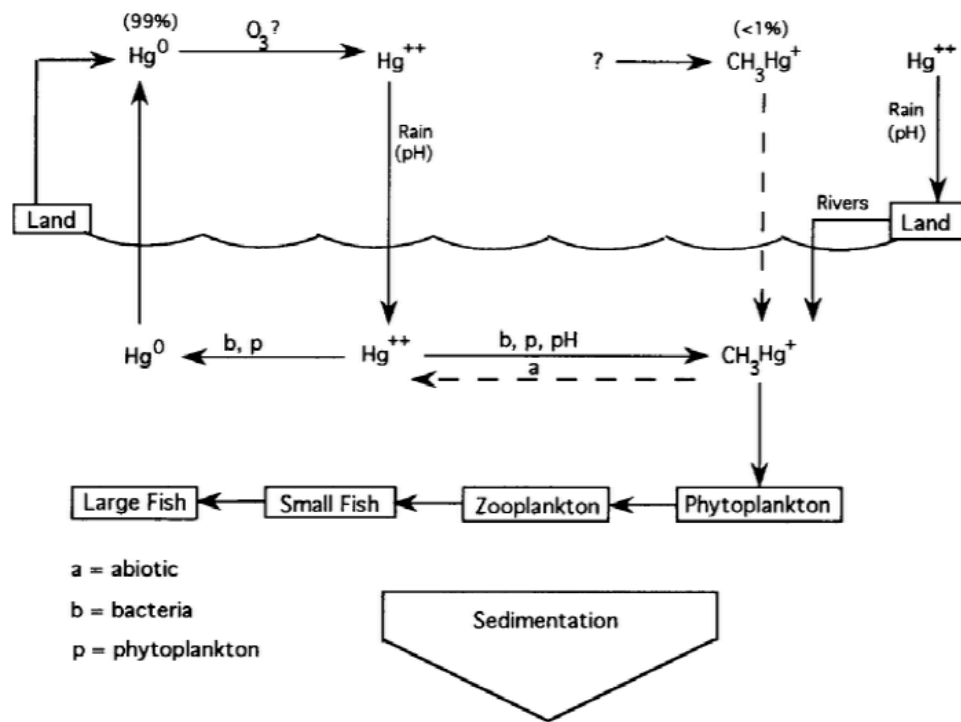


Fig 2. Current model of the global and chemical cycle of mercury (Clarkson 1998)

Dated back to the Archean time, it is believed that  $Hg^{2+}$  transfers to MeHg under the assistance of methanogenic bacteria, creating a protective mechanism for the early appeared cells in evolution. However, when the organisms evolved to a certain form which depends a central nervous system for living, this protective element for simple cells becomes a threat which is harmful to a more complex life form. As the evolution continues, MeHg coming from  $Hg^{2+}$  from freshwater or seawater by methylation is the main source of human exposure. The major reason of this is the bioaccumulation in the aquatic primary producers and consumers as well as the biomagnification along the trophic food chain, from the aquatic ecosystem to human beings. MeHg does not damage all parts of the central nervous system in the brain; however, it has selectivity. Normally, in adult humans, it is more

likely to focus on the specific cell types located in a certain anatomical area. For example, the visual cortex and the cerebellum are the common targets. During the prenatal period, the exposure of MeHg is more possible to disrupt the normal development of a fetal brain. Besides, during pregnancy, too much exposed to MeHg causes tremendous damage to both the pregnant mother and infant (Clarkson 1998).

## **2.3 Traditional methods for determining Hg<sup>2+</sup>**

### **2.3.1 Atomic optical spectroscopy**

Atomic optical spectroscopy can be divided into two main kinds, which are atomic absorption spectroscopy and atomic emission spectroscopy (Liu 2005). It is an important method to achieve micro-analysis. Different chemical elements will have their unique spectra. Based on this theory, atomic optical spectroscopy can be used to identify and quantify different species and quantity of the elements in the sample (Liu 2005). The sample needs to be prepared and sent to an atomizer. The atomizer is a high cost component of the whole device to provide energy, dry vapourize and atomize the prepared sample (Beijing X&D Shuaiyi Technology CO., LTD, China 2012). After being processed by the atomizer, the sample's element component can be detected through a spectra detector.

There are five main methods to complete sample preparation: supercritical fluid extraction (SFE), subcritical water extraction (SWE), accelerated solvent extraction (ASE), microwave assisted technology (MAT), and ultrasound assisted extraction (UAE). SFE is a separation method. Under the supercritical temperature and pressure, supercritical fluid is used as the extracting solvent to extract one component from another solid matrix. This method depends on the high-pressure system, reflux system and extraction column working optimally in the whole device. Therefore, the cost of device

is relatively high. Besides, the optimization of parameters includes density, pressure, temperature, flow-rate, and extraction time, which also incurs a high cost. SWE is a concept about using water as extracting solvent and extracting the organic or metaled-organic compound in the solid or semisolid matrix. This method has high requirement of temperature because high temperature can reduce the polarity of water, which can be used in extracting polar or nonpolar substance. In order to keep this high temperature, more cost should spend on high technology requirements of the device. The main theory of ASE is the same as SWE. However, this method depends on either high temperature or high pressure. Normally, the microwave system installed in the instrument includes high power, which can decompose most of the organic elements in the sample. Therefore, this instrument is suitable for determining the total amount of chemical elements. The extraction efficiency of UAE depends on the stirring strength and the properties of solvents (Sun et al. 1999).

Obviously, although the test process for using spectroscopy is not difficult and the result will come immediately, the sample preparation requires high quality and cost. Despite this, a variety of factors should be concerned, for example, the contamination of the samples or the signals from scattered or stray light, because they can compromise the final data and invalidate the results (Lakowicz 2006). Moreover, the dynamic of the element cannot be observed.

### **2.3.2 Isotopic labeling technique**

Isotopic labeling technique is a method to research the behaviors of chemical elements by mean of adding radioactive isotope or enriched stable isotope tracer as a label to participate in a chemical or physical reaction. For  $\text{Hg}^{2+}$  or

MeHg detection in the aquatic system, radioactive mercury isotopic ( $^{203}\text{Hg}$ ) is normally used (Bao et al. 2013).

Before doing the analysis, the sample should be disposed by some complicated processes. There are three main sample preparation methods: direct dilution, dry ashing and hydro decomposition. Although direct dilution is easy to use, the detection capability of some elements can get worse when doing dilution. Dry ashing can make part loss or total loss of the object metal ions. For hydro decomposition, using concentrated nitric acid under high pressure and temperature is powerful for decomposition (Chen et al. 2000). However, the concentrated nitric acid has strong oxidizing property and it can damage not only the sample's structure but also the skin or other facial tissues. Under high pressure and temperature, the cost of the analysis will increase and the training of the technicians should upgrade.

The amount of this tracer located in the environmental media can be used to calculate the amount of transportation and transformation of a specific chemical element. Besides, the use of a radioactive mercury isotopic label should have some limitations. Firstly, commercial  $^{203}\text{Hg}$  has low reagent purity and radioactivity. The amount of the mercury isotopic added in the environment can be much higher than those originally exist in the environment, which can disturb the original ecosystem, inhibit the activity of mercury sensitive organisms and stimulate propagation of mercury-resistant organisms. As a result, this can accelerate the methylation of inorganic mercury ion rate. Moreover, the radioactive mercury isotopic is not environmental friendly because of its radioactive contamination. This method should complete under the strict experimental conditions and require high level for the technicians (Bao et al. 2013).

### **2.3.3 Enzymatic inhibition**

After the  $\text{Hg}^{2+}$  combines with mercapto and methyl mercapto to form the active center of the enzyme, and this component can change the structure and property of enzyme active center. In this case, the activity of enzyme is going to decrease. As a result, it can change the colour of chromophores, pH-value, conductivity and absorption intensity in the substrate-enzyme system. From detection of these changes, the quantity of  $\text{Hg}^{2+}$  can be analyzed (Sun et al. 2012). Once the water sample is obtained, it should immediately be sent to the laboratory and filtered twice to avoid any contamination. Besides, the water sample should store at  $-20^{\circ}\text{C}$  (Deshpande 2010). This sample preparation will also limit the testing condition, and make the detection inflexible. Moreover, the enzyme, as a bio-tracer, has its own activity, which is also a factor influencing the sample analysis. Also, the sensitivity of enzyme is a factor that should be considered (Shukor et al. 2009).

### **2.3.4 Inductively coupled plasma mass spectrometry**

Inductively coupled plasma mass spectrometry (ICP-MS) is able to detect both metal and non-metal ions at a very low concentration. This process can be completed by ionizing the sample with inductively coupled plasma. After that a mass spectrometer is used to separate and quantify the ions. ICP-MS can provide high speed, precision and good sensitivity (Lin et al. 2004). Chiou et al. (2001) used a vapor generation system and LC with combination of ICP-MS to determine mercury in biological tissues. Another study (Allibine et al. 1998) also used ICP-MS with addition of gold to the potable water samples to determine mercury micro-quantity. However, it also has its own disadvantages. A lot of interference can be introduced to the determination process, such as argon, which is the chemical element from the plasma, the component gases of air leaking through the con orifices, also the

pollution caused by glassware and the cones (Chen et al. 2000). Another demerit is that the detection of ICP-MS needs to use at least 5 mL of the solution. If the sample solutions does not satisfy the requirement, they need to be diluted to the lowest testing volume. It is also an important factor to affect the final result, which can introduce error.

It is considered that these four methods for mercury ion detection are reasonable and all of them have their own advantages. These methods can well achieve qualitative and quantitative analysis. However, compared to the fluorescence probes, in particular AIEgens, these methods are not able to determine the dynamic of  $\text{Hg}^{2+}$  in an organism. Also, these methods are complicated in sample preparation as they require high cost, long time, and highly skilled technicians. In addition, they have various sensitivity in different probes and are not environmental friendly. As the conventional method to determine mercury concentration in solution state, one of the introduced traditional methods, ICP-MS has been applied to compare with the AIE method developed in this thesis.

## **2.4 Novel methodology---- Fluorescent probes**

Fluorescent probe as a novel method in the field of biological, chemical, biomedical and environmental sciences, not only has qualitative and quantitative detection, but also provides a direct way to visualize and monitor the complicated biological structures and processes in a living organism on site. Nowadays, a large number of fluorescent sensors and probes are used for detecting small molecules, polymeric materials, nanoparticles and dosimeters, which are powerful and useful tools and indicators for the contemporary studies (Jiang et al. 2016).

### **2.4.1 Aggregation-caused quenching (ACQ)**

A qualified fluorescent probe should have high sensing and imaging sensitivity which are determined by the brightness of the fluorescent probe as well as the contrast of its fluorescence before and after analyte binding. However, a lot of fluorogens, with the pi-pi stacking structure, have the same problem called aggregation-caused quenching (ACQ). They usually quenched at a high concentration or in an aggregated state. Although these fluorescent probes have high emission in the solution state, in the aggregated state, they perform weak emission or even non-emission. This effect also has an opposite influence of bioanalytes because of a great limitation for the labelling degrees of fluorophores. Besides, researchers are pushed to use the probes in the diluted solution, which causes a great difficulty to analyse the molecule. In addition, it is likely to cause ACQ effect in the dilute solution because the fluorophores have the tendency of accumulating in the surface, leading to the high concentration in the particular area. This is the reason why most fluorescent probes have low efficiency and operate in a ‘turn-off’ mode with a narrow scope of practical applications (Ding et al. 2013, Jiang et al. 2016).

### **2.4.2 Aggregation-induced emission (AIE)**

Compared to the ACQ fluorogens, aggregation-induced emission fluorogens (AIEgens) are more powerful as they perform high emission in the aggregated state, which gives a straightforward solution to deal with the ACQ problem. The AIEgens have different molecule structures compared to the ACQ fluorogens. The typical structure of AIEgens is a propeller-shaped rotor like. The connection of benzene is a carbon-carbon single bond between benzene instead of connecting with the pi-pi stacking (Fig. 3). This structure enables AIEgens undergoing low-frequency torsional moment and

this structure preforms as the molecules are isolated. As a result, they are more possible to have low emission in dilute solutions. Whereas, when the AIEgen aggregates, the unique structure restricts the intermolecular rotation, which shows high emission and has strong fluorescence in the aggregated state (Fig. 4). Besides having the qualitative and quantitative detection as well as determining the dynamic of molecules in vivo, AIEgen is more powerful to overcome the problem caused by ACQ fluorogens (Ding et al. 2013, Jiang et al. 2016). The attribution of AIEgens provides a great development of fluorescence light-up molecules and it is a highlight for specific analyte detection and imaging (Ding et al. 2013, Jiang et al. 2016). In the past decade, AIEgens have been widely and successfully used in a certain number of biological applications, like long-term cell tracking, non-self-quenching DNA labeling, inhibition of amyloid fibrillation, differentiation of protein monomers, oligomers and fibrils, monitoring of cell apoptosis and long-term bacterial viability assays (Guo et al. 2015).

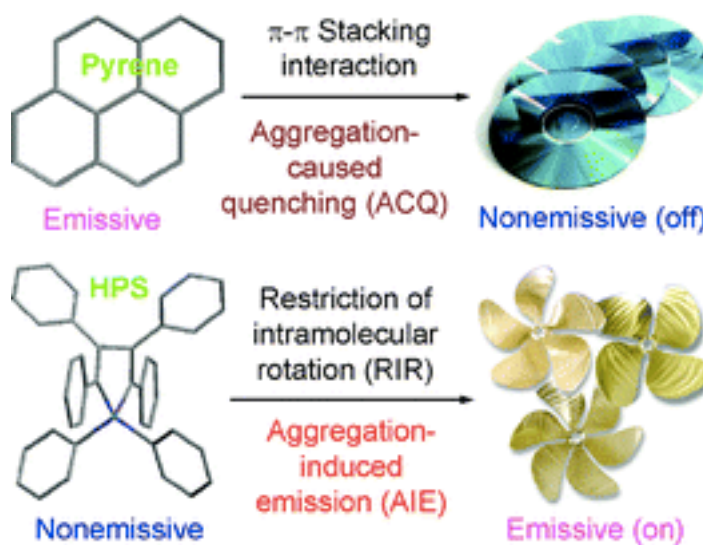


Fig 3. Structure of ACQgen & AIEgen (Hong et al. 2009)



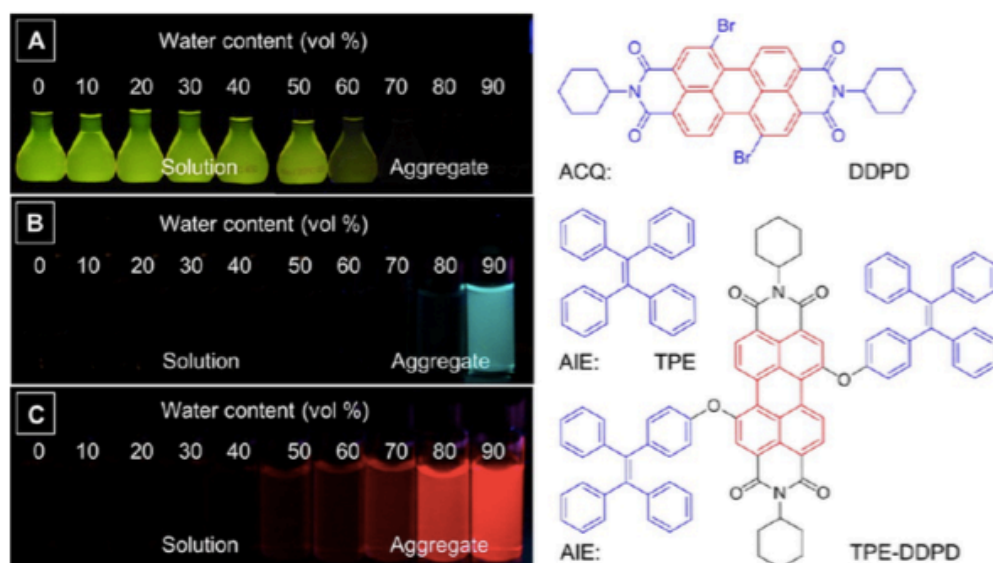


Fig 4. Fluorescence photographs of (A) DDPD with aggregation-caused quenching (ACQ) feature and (B) Tetraphenylethene (TPE) and (C) TPE-DDPD with aggregation-induced emission (AIE) attribute in THF/water mixtures with different water contents upon UV illumination (Ding et al. 2013).

## 2.5 Methods of $\text{Hg}^{2+}$ detection using AIEgens

AIEgens are well performances with the fluorometric sensing of  $\text{Hg}^{2+}$ . This novel detection strategy has thereby attracted growing attention (Zhang et al. 2011).

TPE- functionalized benzothiazolium salt with the counterion iodide (407-I) emits high fluorescence in the solution state, but has low fluorescence in the aggregate or solid state, which is the quenching phenomenon.  $\text{Hg}^{2+}$  is expected to displace the cationic unit of 407-I because of its high affinity towards the iodide. To get a better response, thereby conduct 407-I in the aqueous buffer solution to ensure the initial state is emission-off. When increasing the addition of  $\text{Hg}^{2+}$ , the bright red fluorescence rises as well. This

phenomenon shows that 407-I is able to perform as a light-up probe for  $\text{Hg}^{2+}$  with superb selectivity and specificity. Most importantly, the detected limitation of this simple and economic displacement method can reach  $1 \mu\text{M}$  (Mei et al. 2015).

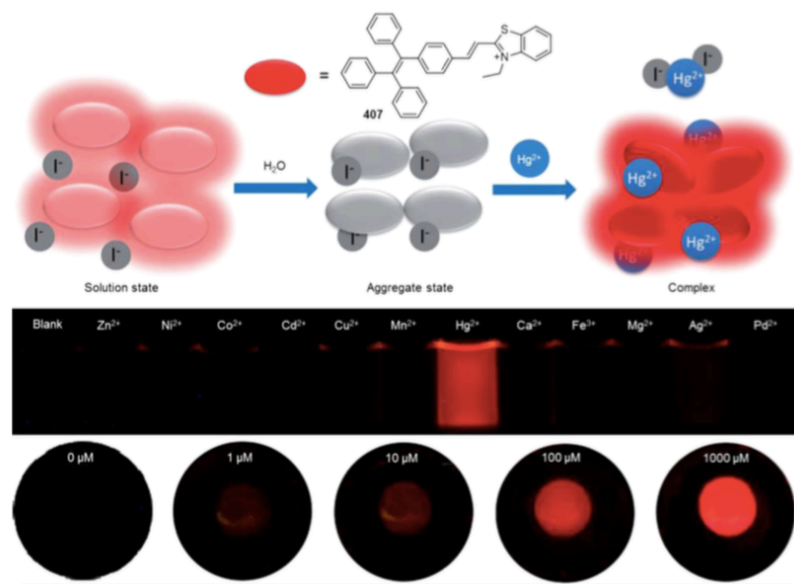


Fig 5 The working mechanism of 407-I fluorescent sensor with  $\text{Hg}^{2+}$ . High affinity test between 407-I and  $\text{Hg}^{2+}$ . Concentration of  $\text{Hg}^{2+}$  affects the red bright fluorescence (Mei et al. 2015).

Because of the strong combining ability to  $\text{Hg}^{2+}$ , which can be a useful strategy in detecting  $\text{Hg}^{2+}$ , the aggregation can be triggered by the coordination between the AIEgen and  $\text{Hg}^{2+}$  and induce the fluorescence response. Another AIEgen 408 (a triphenylamine-triazine motif with two thymine groups), emitting red fluorescence in aggregate state, is used as an  $\text{Hg}^{2+}$  detection probe based on the abovementioned principle. The light-up response is owing to the combination of two thymine groups of 408 with  $\text{Hg}^{2+}$ , activating the restrict intermolecular motion process and the AIE phenomenon. Moreover, this special coordination provides high selectivity of 408 and  $\text{Hg}^{2+}$ . Besides, triphenylamine-triazines, other AIEgens containing thymine groups are also used as the turn-on detection of  $\text{Hg}^{2+}$ ,

which means using AIEgen to detect  $\text{Hg}^{2+}$  can become a universal method (Mei et al. 2015).

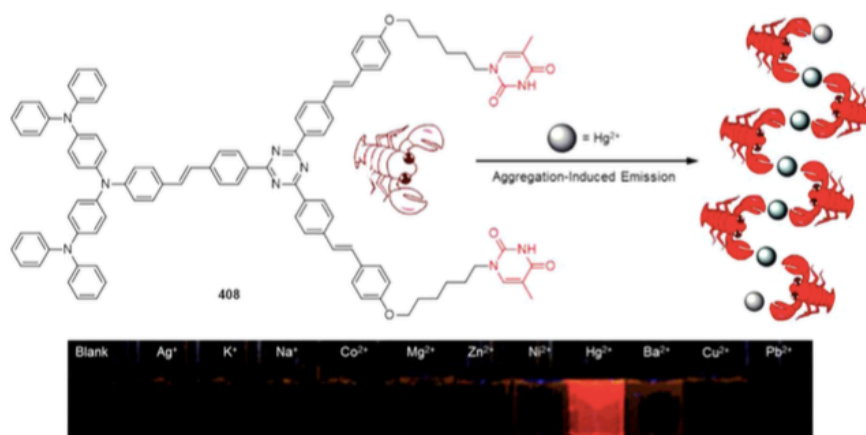


Fig 6 The working mechanism of 408 fluorescent sensor with  $\text{Hg}^{2+}$ . High selectivity between 408 &  $\text{Hg}^{2+}$  (Mei et al. 2015).

Except for combining with the thymine group, imine is another strong functional group coordinating with  $\text{Hg}^{2+}$ . The structure of this AIEgen is similar to the material of 409 AIEgen (Fig 7). For this structure, increasing the concentration of  $\text{Hg}^{2+}$  can also enhance fluorescence. The fluorescence intensity is 7.6% in the low aggregated state, but that rises nearly 10 times when the addition of  $\text{Hg}^{2+}$  reaches 100  $\mu\text{M}$ . For this special structure, AIEgen 409 can detect a very limited amount of  $\text{Hg}^{2+}$  with only 4.5 nM and has powerful selectivity to  $\text{Hg}^{2+}$ . This combination characteristic of recognition moiety connecting with AIEgen provides highly adaptable and flexible strategy in detecting  $\text{Hg}^{2+}$  (Mei et al. 2015).

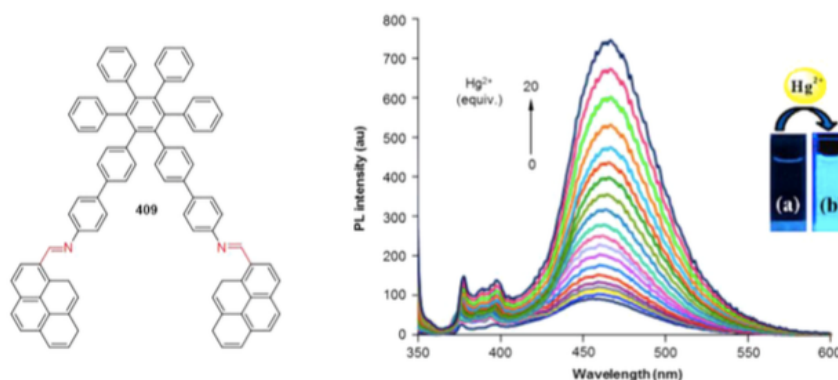


Fig 7 Molecular structure of 409 AIEgen. Fluorescence in different  $\text{Hg}^{2+}$  intensity (Mei et al. 2015).

Additionally, using the solubility change strategy in the hydrophilic AIEgen is also effective in detecting  $\text{Hg}^{2+}$ . AIEgen 410 is an example. This AIEgen 410 shows nearly non-luminescent in aqueous solution because of the active intermolecular motion. Under the reaction of  $\text{Hg}^{2+}$ , the 410 AIEgen can be transformed selectively into the 338b AIEgen which is hydrophobic. Hence 410 can perform the fluorescence turn-on probe for  $\text{Hg}^{2+}$ . Besides, increasing the concentration of  $\text{Hg}^{2+}$  can also increase the fluorescence intensity. This strategy can reach the detection limit of  $0.1 \mu\text{M}$  of  $\text{Hg}^{2+}$  and have an outstanding selectivity. The most essential factor of this strategy is that it is able to do the sensing of  $\text{Hg}^{2+}$  in the living cells with turn-on fluorescence (Mei et al. 2015).

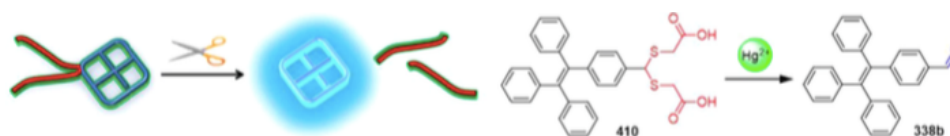


Fig 8. Schematic illustration of the fluorescence “turn-on” chemosensor (410) for  $\text{Hg}^{2+}$  detection based on the polarity and solubility change (Mei et al. 2015).

With the same recognition moiety and signaling motif, the sensing behavior can also change if the molecular design or experimental conditions are different. AIEgen 411 has the same carboxylic groups, which is the recognition moiety. This is similar to 410 but it uses a different strategy in fluorescence. If use the medium contains iron (III) as well as  $\text{Hg}^{2+}$  to improve its hydrophobicity, these carboxylic groups can react with the metal ions first and change to an intermediate product. This intermediate product is able to recognize  $\text{Hg}^{2+}$ . Carrying 4 carboxylic groups make AIEgen 411 less possible to dissolve completely in water, performing a strong emission

because of its large hydrophobic fragment. The emission can be turn-off when iron (III) is added into the water containing AIEgen 411. Under this off-state solution [411-iron (III) complex],  $\text{Hg}^{2+}$  is able to be detected sequentially and change the fluorescence into a turn-on mode. In order to enhance fluorescence, increasing  $\text{Hg}^{2+}$  addition is easily to generate higher concentration of hydrophobic 412 and form aggregates, since this action can restrict the intramolecular motion of the signaling motif (TPE unit). The arising 411-iron (III) complex provides a wide-range pH detection of  $\text{Hg}^{2+}$ , excellent selectivity and appreciable sensitivity in the water (Mei et al. 2015).

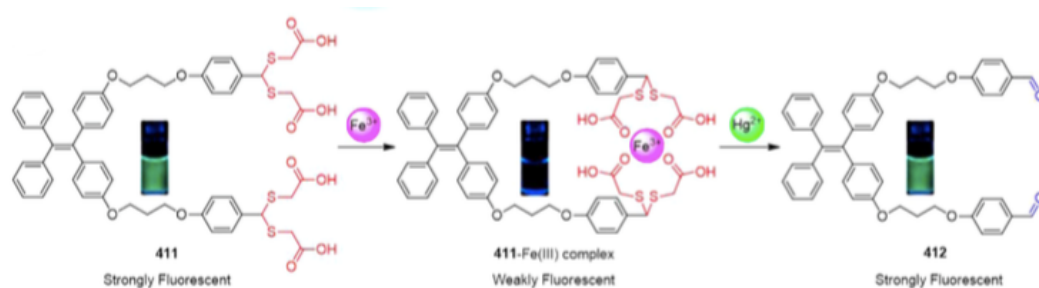


Fig 9. Fluorescence “on–off–on” chemosensor (411) for sequential recognition of  $\text{Fe}^{3+}$  and  $\text{Hg}^{2+}$  in water (Mei et al. 2015).

A novel strategy called dark through-bond energy transfer (DTBET) process is used as an improvement to construct ratiometric  $\text{Hg}^{2+}$  sensors with high performance. TPE derivatives are used as an absorption dark donor because of their AIE characteristics. These TPE derivatives have high recognition of  $\text{Hg}^{2+}$ . Only blue emission of the TPE aggregate occurs when  $\text{Hg}^{2+}$  is absent. After different concentration of  $\text{Hg}^{2+}$  is added, it triggers the generation of rhodamine fluorophores and improve the solubility in water (Fig. 10). Consequently, because of the DTBET process, it is impossible that the TPE emission can be observed. Furthermore, it is more likely to intensify the non-radiative decay while emission of rhodamine. Therefore, ratiometric  $\text{Hg}^{2+}$  detection can be achieved. For getting better fluorescence performance,

the system should be recorded in a CH<sub>3</sub>CN/H<sub>2</sub>O mixture (volume of CH<sub>3</sub>CN /volume of H<sub>2</sub>O = 2:3), because the PL intensity at 480 nm reaches a maximum at 60% water fraction (Chen et al. 2017).

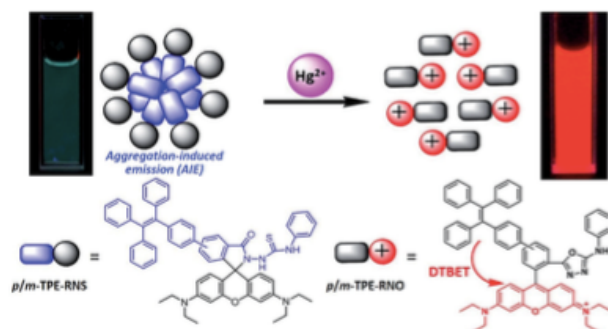


Fig 10. Mechanism of TPE derivatives reacting with ratiometric Hg<sup>2+</sup> (Chen et al. 2017).

## 2.6 Use AIEgens for aquarium system

A recent study (Wang et al. 2014) used TPE-AmAl, the AIEgen, to dye the lipid droplets (LDs) in living cells as well as in green algae. Because of the special characteristic of cell-permeable, TPE-AmAl can accumulate in LD selectively and perform an efficient dyeing.

In addition, TPE-AmAl can be used *in vivo*, in green algae. To understand the value of algae, determining the content of its lipids is an effective way. The use of TPE-AmAl to indicate the LDs in algae is a novel approach. Although the chloroplast can also emit red colour in the image, it is not a disturbance for determining the LDs content because it can be differentiated by greenish blue emission (Wang et al. 2014).

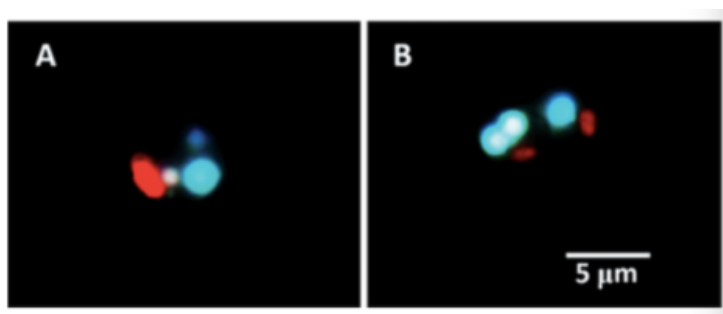


Fig 11 Green algae stained with TPE-AmAl in fluorescent images. Blue colour emitted from LDs, and red colour emitted from chloroplast (Wang et al. 2014).

From the abovementioned studies, Wang and his team members concluded that TPE-AmAl, as an AIEgen, is an effective dye and can be used in an aquatic system.

Ruan et al. (2015) has designed a novel  $\text{Hg}^{2+}$  chemodosimeter called TPE-S, which is an AIEgen. In order to understand the multistage amplifying effect, the  $\text{Hg}^{2+}$ -promoted reproduction reaction was coupled with ketone-enol isomerization. The changes are able to notify immediately from the colour and fluorescence. Besides, this TPE-S has a high selectivity for  $\text{Hg}^{2+}$  detection. The test covered detections of other metal ions such as  $\text{Ag}^+$ ,  $\text{Fe}^{3+}$ ,  $\text{Cu}^{2+}$ ,  $\text{Pb}^{2+}$ ,  $\text{Co}^{2+}$ ,  $\text{Cr}^{3+}$ ,  $\text{Al}^{3+}$ ,  $\text{Cd}^{2+}$ ,  $\text{Mg}^{2+}$ ,  $\text{Mn}^{2+}$ ,  $\text{Ba}^{2+}$ ,  $\text{Fe}^{2+}$ ,  $\text{Ca}^{2+}$ ,  $\text{Ni}^{2+}$ ,  $\text{Zn}^{2+}$ ,  $\text{Li}^+$ ,  $\text{K}^+$  and  $\text{Na}^+$ , and none of them presented inference to the  $\text{Hg}^{2+}$  sensing process. Furthermore, TPE-S was applied for making test strips, which have the similar usage as the pH-indicator paper. The colour of the paper showed an instant change. When the  $\text{Hg}^{2+}$  concentration in the water increases, the colour of test strips changes from the light brown to dark brown and then to light purple and finally to dark purple. The water samples also show this tendency. From Fig. 12, it is shown that the testing limit was  $1 \times 10^{-7}$  M  $\text{Hg}^{2+}$  concentration in the water solution, which means the sensitivity is quite high. This AIEgen presents the high selectivity and sensitivity for detecting

Hg<sup>2+</sup> in the water. Besides, the test strip detection was the spotlight of the convenient detection of Hg<sup>2+</sup>.

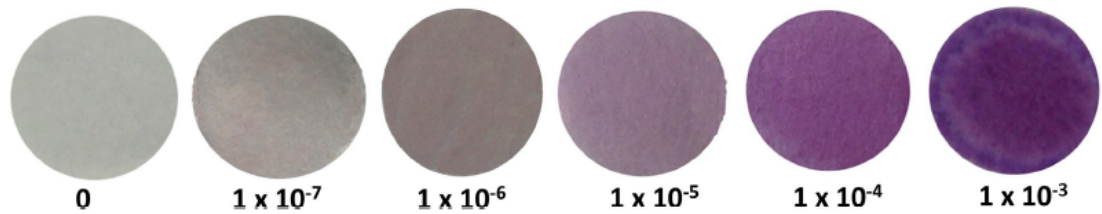


Fig.12 Test strips of indicating different Hg<sup>2+</sup> concentrations (Ruan et al. 2015).

Another recent study (Guo et al. 2015) used AIEgens as a biomarker to detect the viability of microalgae in aquatic ecosystems. Microalgae play an important role to the aquatic food web. Because of the special characteristics----ubiquitous, cost saving and sensitive to chemical change in the atmosphere, microalgae are widely used in determining the contamination index of the water system. Therefore, the viability determination of the microalgae is an important factor to indicate whether the aquatic ecosystem is polluted or not. In this study, *Nannochloropsis oculata* (*N. oculata*), a unicellular organism with spherical shape and 2-5  $\mu\text{m}$  diameter' long, is used to do the test. Because of its high quantum efficiency, good biocompatibility and appreciable photostability, AIEgen fluorescence becomes a novel method to use as a biomarker. An AIE-active molecule is discovered in their study, which is 1,2-bis [4-(3-sulfonatopropoxy) phenyl]-1,2-diphenylethene salt (BSPOTPE). What they found important is that BSPOTPE holds an increasing trend of fluorescence at the BSPOTPE concentration of 200  $\mu\text{M}$  in the living *N. oculata* whereas the dead *N. oculata* remains a stable emission. It is quite significant that the living and dead *N. oculata* show different fluorescence.



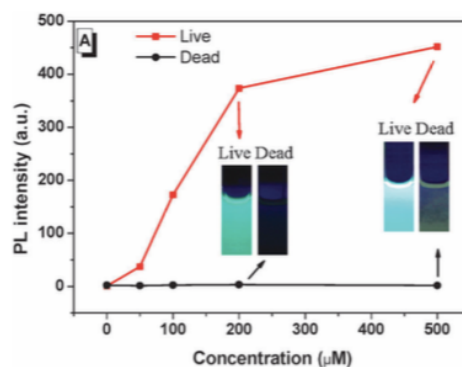


Fig 13. Different fluorescence of various concentrations between living and dead *N. oculata* (Guo et al. 2015).

Besides, this AIEgen binding with *N. oculata* shows no overlap with the auto-fluorescence of chlorophyll staining in the microalgae. Moreover, the fluorescence of living cells binding with BSPOTPE can be observed clearly; whereas the dead *N. oculata* cells have nearly non-emission after being bound by the AIEgen.

Jiang et al. (2016) and his team members used a novel AIEgen (m-TPE-RNS) to understand the complicated bioaccumulation process by monitoring and quantifying in a microcosm aquatic ecosystem. Firstly, they chose certain amount of the heavy metal pollutant which is  $\text{Hg}^{2+}$ , and a primary producer, the *E. gracilis* representing a common algal species in fresh water. As owning the 'turn-on' feature, the AIEgen is easy to complete the detection of the  $\text{Hg}^{2+}$  in the aquatic environment. The photoluminescence (PL) intensity was used to build the relationship between the concentration of AIEgens and  $\text{Hg}^{2+}$ . Knowing the PL intensity of the solution, with the assistance of the standard curve, the concentration of the  $\text{Hg}^{2+}$  in the bioaccumulation process is easy to be quantified.

Using different equations to calculate bioaccumulation ( $A_t$ ), bioaccumulation efficiency ( $E_t$ ) and bioaccumulation ratio ( $R_t$ ) of  $\text{Hg}^{2+}$  in algae is easy to

know that bioaccumulation process depends on time and the concentration of  $\text{Hg}^{2+}$ .

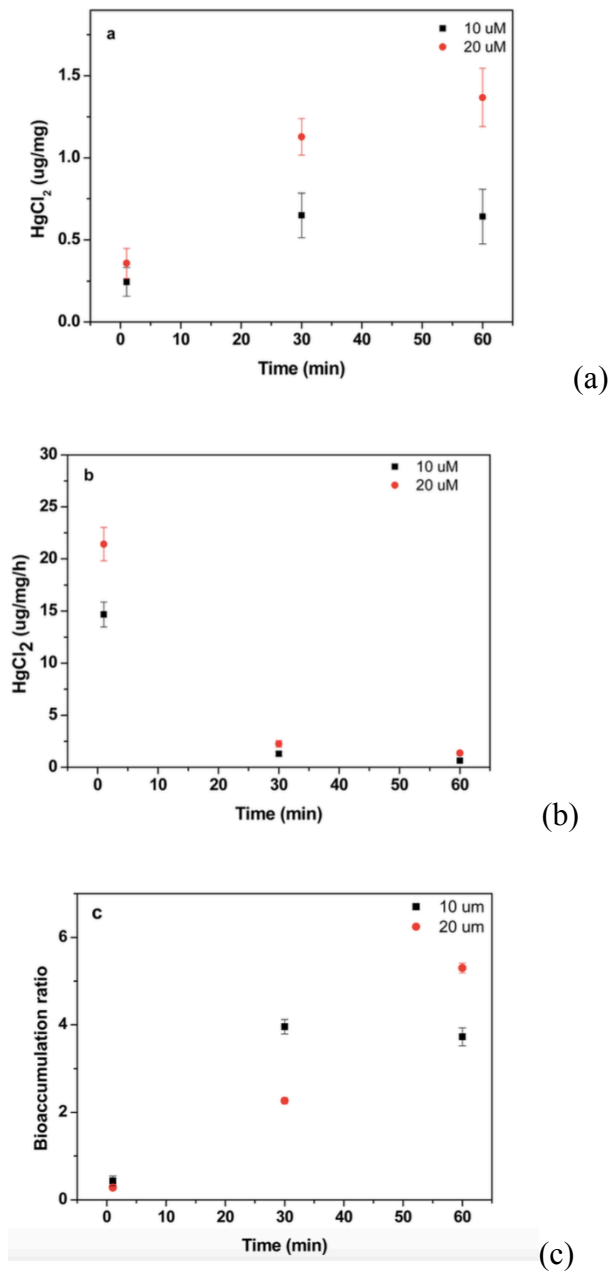


Fig 14. (a) Amount of bioaccumulation, (b) bioaccumulation efficiency, and (c) bioaccumulation ratio of *E. gracilis* at different  $\text{Hg}^{2+}$  concentrations over time (Jiang et. al 2016).

Additionally, they also proved that algae density is also an important factor influencing the bioaccumulation process. In a fixed period, the algae density and the amount of bioaccumulation have positive correlation, which means

that the increase of the algae density is going to raise the amount of bioaccumulation.

This method is also useful for tracking the dynamic of the bioaccumulation process, observing the processes of absorption and release of  $\text{Hg}^{2+}$  in the algal cell.

## 2.7 Daphnia

*Daphnia* is one of the important species in the aquatic system because of its role as an herbivore to transfer energy from a lower trophic level to a higher level. Due to its high adaptability, daphnia is suitable for living in various aquatic environments, such as freshwater lakes, ponds, creeks and rivers. It also plays a significant role in the food chain in aquatic systems. *Daphnia*, which is the typically filter feeders, ingesting unicellular algae and some kinds of bacteria (Gliwicz 2008) and is a high quality fish food.

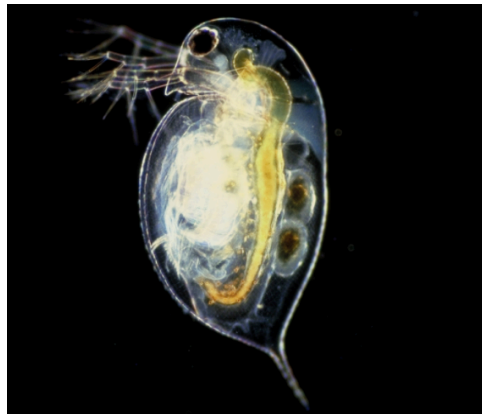


Fig 15. The transparent body structure of *Daphnia* (Heber 2005)

### 2.7.1 The status of *Daphnia* in the trophic level of the aquarium system

The *Daphnia* plays an important role in freshwater systems. This organism can be found commonly in the lacks, creeks or rivers. Besides that, it is a

significant trophic bond to link phytoplankton and fish. The body size of daphnia is relatively large, which means that it is easy to carry higher amount of  $\text{Hg}^{2+}$  than other zooplankton species at the same trophic level. Therefore, daphnia can be a good predictor of detecting  $\text{Hg}^{2+}$  in the culture medium (Tsui & Wang 2004).

### **2.7.2 Morphological structure of daphnia**

The size of a daphnia is usually 1 to 5 mm long, which is larger than many other zooplanktons. With its transparent body, it can be easily observed under an optical microscope. Different organs are able to be seen through the transparent body carapace. Therefore, the ingesting process and digesting mechanism is easy to be observed (Ebert 2005).

### **2.7.3 Mercury toxicity experiment in daphnia**

Wim and Colin (1997) used five different digestive enzymes from *Daphnia* as indicators to quantify the response of *Daphnia* after 48 and 96-hour exposures to different sublethal concentrations of mercury chloride ( $\text{HgCl}_2$ ). The result showed that from a very low to a high concentration of  $\text{HgCl}_2$  ( $1.8 \mu\text{g/L}$  to  $30 \mu\text{g/L}$ ) in 48 hours, some enzymes' ability decreased, while some showed a U-shape response because of detoxification. For the high concentration of  $\text{HgCl}_2$  ( $30 \mu\text{g/L}$ ) in 96 hours, none of the enzymes was alive. The  $\text{HgCl}_2$  can affect the activity of the digestive enzymes in daphnia through the exposure time and mercury concentration. There are limited studies that used *Daphnia* as the object representing for the zooplankton trophic level in the aquatic system. Therefore, in this thesis, the *D. carinata* was selected as the experimental object.

## 2.8 Literature review summary

It is easily for the organic and inorganic  $\text{Hg}^{2+}$  to pollute an aquatic system. With high pollution,  $\text{Hg}^{2+}$  has high possibility to bioaccumulate in aquatic organisms at different trophic levels. Therefore, it is essential to understand the bioaccumulation process in small aquatic organisms. The qualitative and quantitative detection can be achieved with four conventional methods which are atomic optical spectroscopy, isotopic labeling, enzymatic inhibition and ICP-MS. However, these four methods are not able to determine the dynamic of the  $\text{Hg}^{2+}$  inside an aquatic organism. Therefore, a novel method, which is the fluorescent method, was introduced to overcome this problem. In order to solve the ACQ phenomenon caused by some fluoregens, the AIEgens were used instead. The AIEgens can overcome ACQ and have high emission in the aggregated state because of its special structure and chemical property. Hence, different types of AIEgens can be introduced to combine different ions and have various colour emissions. Many of them are achieved in aquatic organisms to detect some materials,  $\text{Hg}^{2+}$  or other heavy metals. Obviously, because of its effectiveness and simple operation, using AIEgen in detecting the materials and ions in aquatic organisms would be a reasonable and promising method in the future.

## 3. Aim

The bioaccumulation of toxic substances, like  $\text{Hg}^{2+}$  in the aquatic system is a huge problem affecting both environment and organisms' health. Some researchers have already focused on detecting  $\text{Hg}^{2+}$  in the aquatic ecosystem by using AIEgens. However, most of their research and studies are not clear about how the dynamic of toxic substance can transfer inside the organism. In my project, the m-TPE-RNS AIEgen is used to effectively detect bioaccumulation of  $\text{Hg}^{2+}$  in zooplankton, the primary consumer in the

aquatic system. The ratiometric method for  $\text{Hg}^{2+}$  detection is applied, because this method can achieve  $\text{Hg}^{2+}$  detection in a ratiometric way, which means that once knowing the PL intensity ratio in the fluorescent wavelength of a sample, the concentration of  $\text{Hg}^{2+}$  can be deduced from the standard curve accordingly. It is a time and cost effective method to determine the bioaccumulation process inside the aquatic organisms. *Euglena gracilis* (algae) and *D. carinata* (zooplankton) are chosen to perform the primary producer and the primary customer because of their easy collection and culturing as well as low cost. Also, *Daphnia* is easy to observe under the optical microscope and the fluorescence microscope. Use the fix amount of AIEgen to create the standard curve (concentration of  $\text{Hg}^{2+}$  vs. ratio of fluorescent intensity) first and then use this standard curve to determine the absorption of different concentrations of  $\text{Hg}^{2+}$  in daphnia as well as the release rate. By through it, it can be known whether and how much the inorganic  $\text{Hg}^{2+}$  has been bioaccumulated. Before achieving that, the mortality rate and physical response of *D. carinata* to different inorganic  $\text{Hg}^{2+}$  concentration can be used to determine what is the maximum time to cause death. The in situ observation of  $\text{Hg}^{2+}$  dynamic in *D. carinata* can be done by the change of fluorescence with AIEgen with a fluorescence microscope. This can provide a hint on the possible reason for the death of *D. carinata*. Besides, the use of mercury polluted primary producer ---- *E. gracilis* to feed the *D. carinata* can provide information to compare whether the bioaccumulation of heavy metal can be affected through food intake.

## **4. Materials and Methodology**

### **4.1. Materials**

Except for AIEgen (m-TPE-RNS), all reagents were obtained from Sigma-Aldrich Australia and used without further purification. The AIEgen

has been provided by AIEgen Biotechnology, Hong Kong. The mechanism of AIEgen reacts with  $\text{Hg}^{2+}$ , which changes from m-TPE-RNS to m-TPE-RNO with  $\text{Hg}^{2+}$  is shown in Fig. 16 (a).

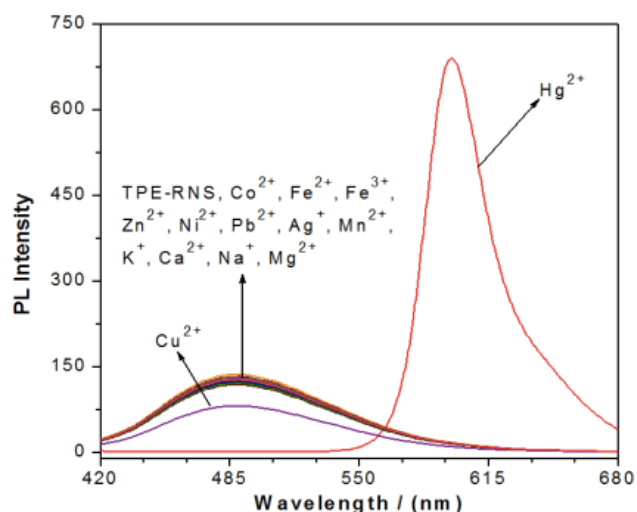
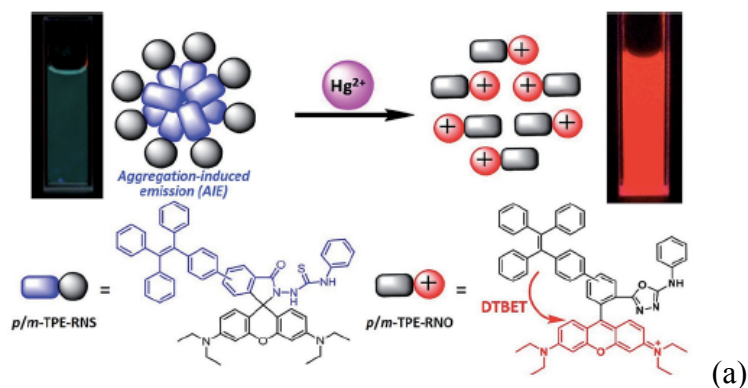


Fig 16 (a) The sensing mechanism of ratiometric  $\text{Hg}^{2+}$  (Chen et al. 2017); (b) PL intensity of 10  $\mu\text{M}$  m-TPE-RNS in  $\text{CH}_3\text{CN}$ -water mixture (60% water fraction) reacting with different metal ions (Jiang et al. 2017).

According to Chen et al. (2017), this AIEgen (m-TPE-RNS) has high selectivity and sensitivity by using the ratiometric method in detection of  $\text{Hg}^{2+}$ . The mechanism of m-TPE-RNS for  $\text{Hg}^{2+}$  was documented by Chen et al. (2017) and shown in Fig 16 (a) as well. Because  $\text{Hg}^{2+}$  was absent from the solution, the hydrophobic sensors are more likely to aggregate in water. In this case, only blue emission of the m-TPE-RNS was observed because of the non-emissive spiro-lactam form rhodamine. After  $\text{Hg}^{2+}$  was added, the

solubility of rhodamine in the solution was improved. Therefore, the fluorescence of m-TPE-RNS was quenched, and the red colour emission appeared, which indicates  $\text{Hg}^{2+}$  in the solution. Fig. 16 (b) shows that m-TPE-RNS has high sensitivity in detecting  $\text{Hg}^{2+}$  compared to other metal ions, which means it is a good dyeing material for detecting inorganic  $\text{Hg}^{2+}$ .

Prepare the stock solution of m-TPE-RNS at 100  $\mu\text{M}$  by dissolving the solid weighed AIEgen in acetonitrile (ACN). This solution needs to be stored in a tinfoil-covered sealed bottle at 4°C in the refrigerator before use. Prepare the stock solution of  $\text{HgCl}_2$  at 1.0 mM and 1  $\mu\text{M}$  by dissolving  $\text{HgCl}_2$  in Milli Q water. This solution needs to be stored in a clear sealed bottle at 4°C in the refrigerator before use.

The *D. carinata* with mean length of 0.8–1.0 mm were obtained from the College of Sciences and Engineering at Flinders University and cultivated in aquarium tanks. The culture medium was prepared by using natural water in Flinders Lake. Micro-*E. gracilis* and baker's yeast were provided to enhance the biomass of the *D. carinata* (over 20-30 ind/L). The aquarium tanks were put into a thermostatic chamber and provided continuing oxygen. To prevent the interference of the chlorophyll in algae, baker's yeast was used to feed the *D. carinata* before the experiment day. The baker's yeast stock suspensions were dissolved of 3 g dry baker's yeast in 60 mL milli Q water and stored at 4°C in the refrigerator. The density of the *D. carinata* can be calculated under naked eyes on an optical microscope (Leica, USA).

By using the experience of incubating algae by Jiang et al. (2016), *E. gracilis* (15-20  $\mu\text{m}$  long and 8-10  $\mu\text{m}$  in diameter) were also obtained from the College of Sciences and Engineering at Flinders University. The culture medium included 30 g wheat grains, 25 g rice grains and 5 g skim milk powders in to 2 L Milli Q water. After boiling at 100 °C for sterilization, the culture medium was stores at 4 °C in the refrigerator before use. *E. gracilis*



were inoculated into the culture medium in 250 mL Erlenmeyer flasks in a thermostatic chamber at 25 °C. Continuous illumination of the thermostatic chamber was controlled at 70  $\mu\text{Mol photons/m}^2/\text{s}$ . The Erlenmeyer flasks were continually provided oxygen by an air pump and stirred manually twice a day to maintain the viability of *E. gracilis* and prevent it from settling at the bottom. A haemocytometer was used to determine the density of *E. gracilis* cells.

## **4.2 Methodology**

### **4.2.1 Developing the standard curve of $\text{Hg}^{2+}$ concentration vs. photoluminescence (PL) intensity ratio using the ratiometric method**

The AIEgen can get the greatest PL intensity at the water volume fraction ( $f_w$ , vol%) of 3:2 in water: ACN.. The m-TPE-RNS and m-TPE-RNO have the PL peak intensity at 480nm and 595nm respectively, and the ratio at 595 nm and 480 nm ( $I_{595}/I_{480}$ ) was obtained to calculate  $\text{Hg}^{2+}$  concentration (Chen et al. 2017). Besides, the standard curve was developed to indicate the relationship between the  $\text{Hg}^{2+}$  concentration and the PL intensity ratio. The PL intensity was determined by a fluorescent spectrometer (Agilent, Varian, Australia), with the excitation wavelength at 350 nm. To develop the standard curve of  $\text{Hg}^{2+}$  concentration vs. PL intensity ratio, a series of different  $\text{Hg}^{2+}$  concentrations (0, 2, 4, 6, and 8  $\mu\text{M}$ ) were used at a fixed AIEgen concentration of 10  $\mu\text{M}$ . The choice of this fixed concentration was based on the result of Jiang et al. (2016) in detecting  $\text{Hg}^{2+}$  concentration.

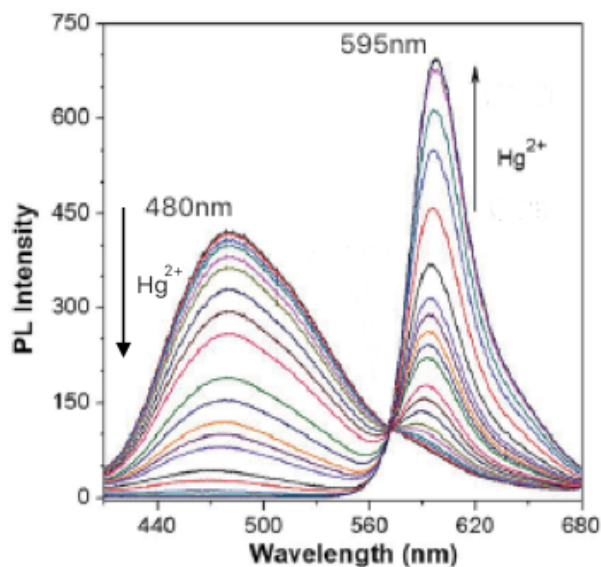


Fig. 17. PL spectra of 10 mM m-TPE-RNS in a CH<sub>3</sub>CN/water mixture at 60% water fraction in the presence of different amounts of Hg<sup>2+</sup> with excitation wavelength of 350 nm (Chen et al. 2017).

#### 4.2.2 The response to different inorganic Hg<sup>2+</sup> concentration and death rate of *Daphnia carinata* in the toxic heavy metal solution

The same density (7 ind/mL) of *D. carinata* were put into the above-mentioned Hg<sup>2+</sup> concentration (5 and 10 μM) to detect their estimated mortality rate in 5, 10, 20, 30, 40, 50, 60, 90, 120, 150 and 180 minutes, respectively. When all *D. carinata* died, the observation stopped. The mortality rate was counted with naked eyes and the optical microscope was used to determine the response of *D. carinata* to inorganic Hg<sup>2+</sup>. Besides, this process was recorded by images to estimate the mortality rate in every 30 minutes.

### **4.2.3 Determine the quantity of $\text{Hg}^{2+}$ bioaccumulated and bioreleased by *Daphnia carinata***

A known number of *D. carinata* was collected from the aquarium tank by a plankton net (mesh size 50  $\mu\text{m}$ ). After that Milli Q water was used to flush the animals into seven containers with different  $\text{Hg}^{2+}$  concentrations (2.5, 5 and 10  $\mu\text{M}$  at culture medium volume of 80 mL). The density of *D. carinata* in each container was 10 ind/mL. Three of them were used as an experimental group for absorption assay. The other three animals are used as an experimental group for mercury release and the rest was the blank control group (No  $\text{Hg}^{2+}$  was added to the culture medium and only Milli Q water was used).

600  $\mu\text{L}$  water in the absorption group was collected over a series of time (5, 10, 20, 30, 40, 50, 60, 90, 120, 150, 180, 210, 240, 270 and 300 minutes respectively) in to 1.5mL centrifuge tubes. Subsequently, 400  $\mu\text{L}$  dissolved AIE solution was added in each tube to meet the requirement of water: ACN ratio of 3:2. After complete reaction (the PL intensity ratio become equilibrium in 1 hour), the PL intensity of each sample solution was detected on the fluorescent spectrometer (Varian, Australia). Apart from measurement by the AIE method, the concentration of  $\text{Hg}^{2+}$  in the group of 2.5  $\mu\text{M}$   $\text{Hg}^{2+}$  was determined using ICP-MS (PerkinElmer NexION 300, US) to compare with the final results from the AIE method.

The three release groups were placed in the corresponding concentration of  $\text{Hg}^{2+}$  (2.5, 5, 10  $\mu\text{M}$  at the culture medium volume of 80 mL) for absorption in 10 minutes, and then transferred from the toxic solution to the Milli Q water after washing with Milli Q water twice. The 600  $\mu\text{L}$  water was collected from each container in 5, 10, 20, 30, 40, 50, 60, 90, 120, 150, 180, 210, 240, 270 and 300 minutes respectively to 1.5 mL centrifuge tubes.  $\text{Hg}^{2+}$

concentrations of three parallel samples were detected by the AIE method by adding 400  $\mu\text{L}$  dissolved AIE solution in each tube.

#### **4.2.4 $\text{Hg}^{2+}$ dynamics in *D. carinata* by AIEgen visualization in vivo**

*D. carinata* were obtained by using the above-mentioned method, and adjusted the density to 10 ind/mL with Milli Q water. After that inorganic  $\text{Hg}^{2+}$  at the concentration of 2.5  $\mu\text{M}$  was added to cultivate the *D. carinata*. Ten to fifteen *D. carinata* were netted from the solution and sampled in 10, 20, 30, 60, 90, 120 and 150 minutes respectively. Pigmented by stock AIE solution, in which the volume ratio of water and ACN was 3:2 at the concentration of 1  $\mu\text{M}$  afterwards. Then, Milli Q water was used to wash the sample once. The further step was to put the *D. carinata* on the Leica TCS SP5 scanning confocal fluorescence microscope for in vivo imaging. During the imaging process, two channels in the microscope were set up, which are the blue channel (460-500 nm) and the red channel (570-610 nm) with the excitation wavelength at 405nm. The blue channel was used to detect the *D. carinata* incubated with only AIEgen, while the red channel was used to detect *D. carinata* incubated with  $\text{Hg}^{2+}$  and AIEgen.

#### **4.2.5 The response of *Daphnia carinata* to inorganic $\text{Hg}^{2+}$ polluted *Euglena gracilis*.**

*E. gracilis* was obtained from the above-mentioned three water containers. The cell density was adjusted to  $1.0 \times 10^7$  cells/mL in Milli Q water where 5 and 10  $\mu\text{M}$  of  $\text{Hg}^{2+}$  solution was added initially in two containers respectively. Before that the normal cell density of *E. gracilis* in the living condition was counted under the optical microscope with a drop in the haemocytometer (Improved Marienfeld Neubauer, Germany). After

incubating under  $\text{Hg}^{2+}$  for 30 minutes, the *E. gracilis* cells were transferred to several centrifuge tubes. These tubes were centrifuged at 4500 rpm for 1 minute. The supernatant liquid was discarded and the remaining *E. gracilis* cells were fed to *D. carinata* (10 ind/mL). As the *E. gracilis* could release certain amount of  $\text{Hg}^{2+}$  to the Milli Q water, in order to reduce this influence (Jiang et al. 2016), the culture water was taken as little as possible. In this experiment, only 20 mL of water was used to cultivate the *D. carinata*. Besides, the parallel water samples were collected until the *E. gracilis* cells were completely consumed by *D. carinata*. The final  $\text{Hg}^{2+}$  concentration of these samples was measured by the AIE method using the fluorescent spectrometer and the standard curve equation was obtained by the ratiometric PL intensity method.

The remaining *D. carinata* in the contaminated water were taken out to observe under an optical microscope (Leica, USA). In order to compare the result with the direct absorption of inorganic  $\text{Hg}^{2+}$  in the *D. carinata*, the images and videos were recorded in every 30 minutes. Besides, the quantity of living and dead *D. carinata* was calculated as well.

## 5. Results and Discussion

### 5.1 The relationship between PL intensity ratio and $\text{Hg}^{2+}$ concentration determined by ratiometric method.

The m-TPE-RNS displayed strong PL intensity at the wavelength of 480 nm and m-TPE-RNO, which the AIEgen reacted with  $\text{Hg}^{2+}$ , displayed strong PL intensity at 595 nm. In order to determine the equilibrium time of the reaction between AIEgen and  $\text{Hg}^{2+}$ , the first experiment used different known  $\text{Hg}^{2+}$  concentrations (2, 4 and 6  $\mu\text{M}$ ) to estimate the equilibrium

reaction time. The intensity ratio of  $I_{595}/I_{480}$  when the AIEgen concentration was fixed at  $10\ \mu\text{M}$ , and time (in minute) and  $\text{Hg}^{2+}$  relationship is shown in Fig. 18.

The PL intensity ratio ( $I_{595}/I_{480}$ ) leveled off and plateaued after 60 minutes. Hence 60 minute was set as the incubation time in the following experiment.

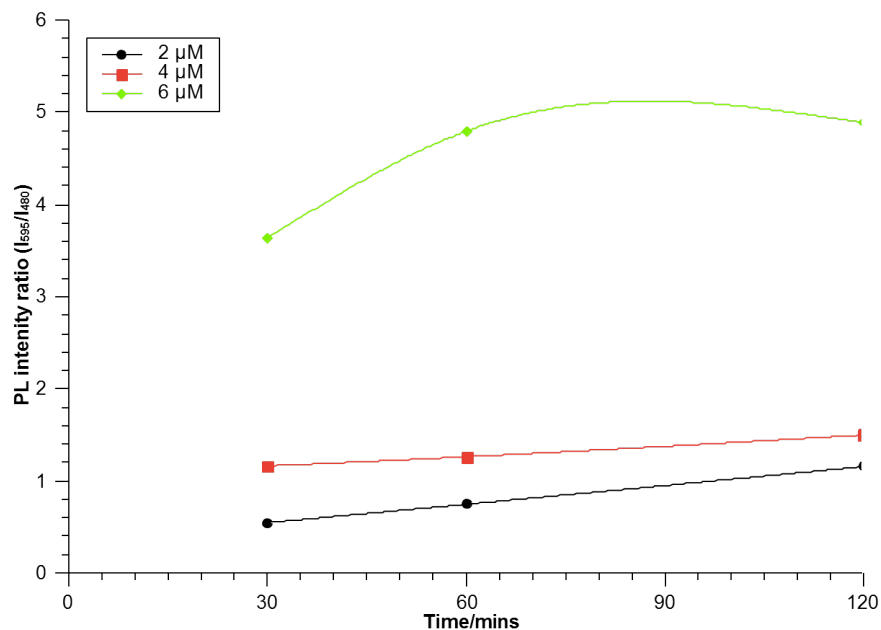


Fig. 18. Relationship between the PL intensity ratio and the incubated time at different  $\text{Hg}^{2+}$  concentrations.

The relationship between PL intensity ratio and different  $\text{Hg}^{2+}$  concentrations with AIEgen concentration in  $10\ \mu\text{M}$  is shown in Figs. 19 and 20. The relationship was built with  $\text{Hg}^{2+}$  concentration less than  $10\ \mu\text{M}$  ( $0, 2, 4, 6$  and  $8\ \mu\text{M}$ ) in 60 minutes. The data were analyzed by SPSS18.0 software and the curve fit result is shown in Table 1 in 60 minutes. From Tables 1 and 2, it is obvious that the logarithmic curve has the highest R square value and lowest standard deviation, which are 0.987 and 0.418 respectively in 60 minutes. Therefore, the standard curve that needs to be chosen is the logarithmic curve. The final applied standard curve equation is Equation (1).

$$C_{(\text{Hg}^{2+})} = 1.569 \ln(\text{PL intensity ratio}) + 1.202 \text{-----(1)}$$

where  $C_{(\text{Hg}^{2+})}$  is the  $\text{Hg}^{2+}$  concentration in the culture medium.

Function	R	R <sup>2</sup>	Adjusted R <sup>2</sup>	Std. Error
Linear	0.898	0.806	0.741	1.609
Logarithmic	0.993	0.987	0.983	0.418
Inverse	0.871	0.758	0.678	1.795
Quadratic	0.969	0.938	0.877	1.111
Cubic	0.985	0.971	0.883	1.081

Table 1. Comparative analysis of five regression functions by SPSS18.0

	Coefficient	Std. Error
$\ln(I_{595}/I_{480})$	1.569	0.104
Constant	1.202	0.264

Table 2. 60 minutes reaction time between PL intensity ratios ( $I_{595}/I_{480}$ ) and different  $\text{Hg}^{2+}$  concentrations.

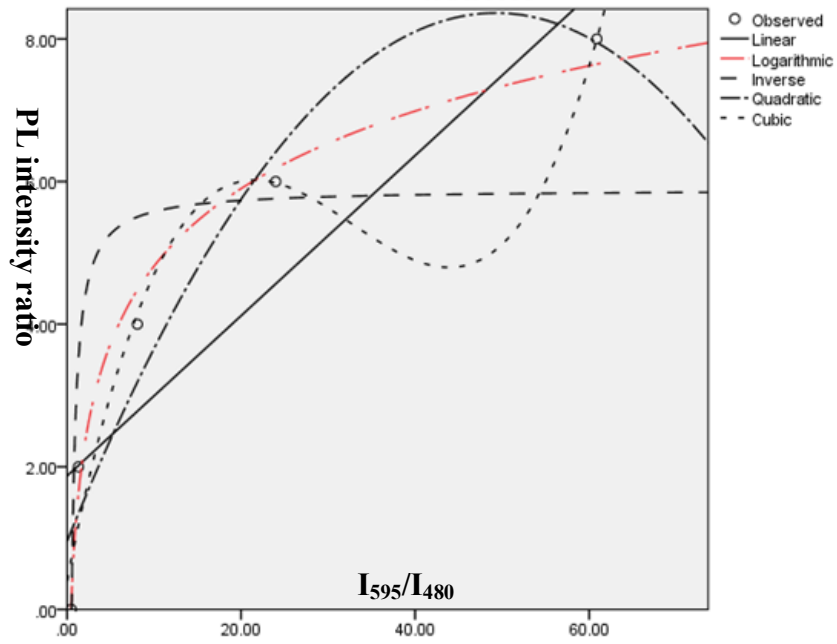


Fig. 19. Five potential curves between  $\text{Hg}^{2+}$  concentrations and PL intensity ratios in 60 minutes.

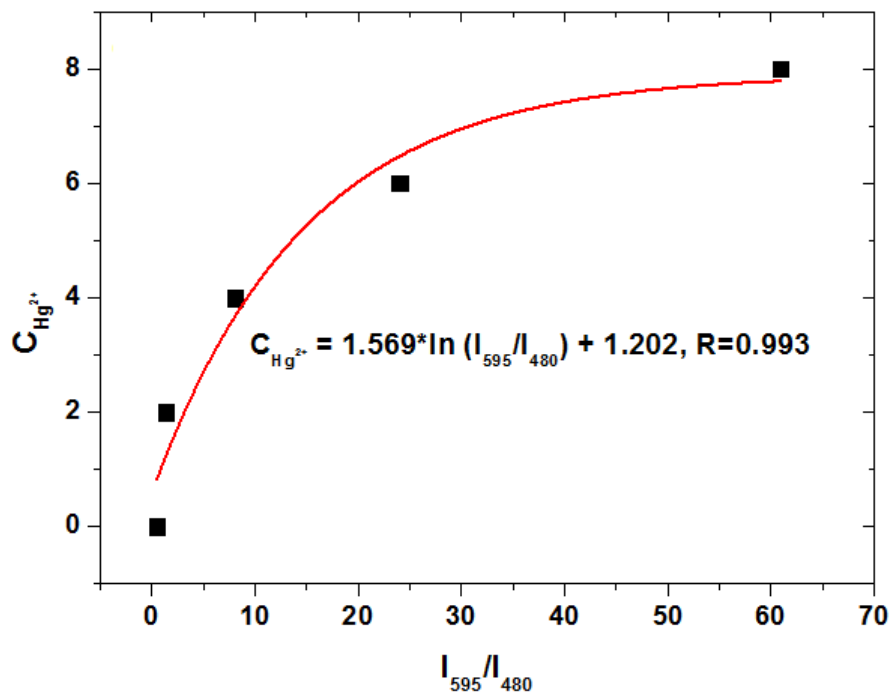


Fig.20 The concentration of  $\text{Hg}^{2+}$  as a function of the PL intensity ratio of  $I_{595}/I_{480}$  and the curve fitting with its equation.



## 5.2 The response of *D. carinata* to inorganic $\text{Hg}^{2+}$ and mortality rate estimation.

The sustainable time of living *D. carinata* at different  $\text{Hg}^{2+}$  concentrations and the response of *D. carinata* to the direct  $\text{Hg}^{2+}$  absorption are the crucial factors for analyzing the process of bioaccumulation in *D. carinata*. The individual *D. carinata* could be observed clearly and easily by using naked eyes. The living *D. carinata* can use their second antenna to stir the water for locomotion. If they sank at the bottom of the culturing containers, they could still move back to the water column. Otherwise, it can be confirmed that those *D. carinata* were dead. In this experiment, two different  $\text{Hg}^{2+}$  concentrations were applied to the culture solution ( $\text{Hg}^{2+}$ ) at 5 and 10  $\mu\text{M}$ . The estimated mortality rate was counted by every 10 minutes in the first hour and then by every 30 minutes with naked eyes. The estimated mortality rate changed over time. The result shows that when the  $\text{Hg}^{2+}$  concentration was at 10  $\mu\text{M}$ , the *D. carinata* started to die from 50 minutes. When the  $\text{Hg}^{2+}$  concentration was at 5  $\mu\text{M}$ , the *D. carinata* started dying from 60 minutes. After tested for 180 minutes, no *D. carinata* in the culture container was still alive. In addition, an interesting phenomenon was noticed. There was a huge amount carapace fallen at the bottom of all culture containers with the tinny larva which dropped from the brood pouch. Fox (1973) described that the carapace included chitinous parts, and the inorganic  $\text{Hg}^{2+}$  can present the chelation with the chitin. As for this, the test extended to 5 hours in the following bioaccumulation and biorelease determination instead of stopping in 3 hours (all the *D. carinata* were dead) to detect whether  $\text{Hg}^{2+}$  concentration would reduce continuously in the culture medium. This is the further result to be confirmed whether parts or all carapaces can be dissolved by inorganic  $\text{Hg}^{2+}$ .

When more *D. carinata* were obtained from the culture medium, and then observed on the optical microscope, it is more clearly to determine the process of the carapace exuviating from the idiosoma or become deformation. Fig. 22 shows that the dying process of the *D. carinata* started from deformation of the carapace. The carapace would become softer than that in the normal organism, which means that it is easy to exuviate. Once the carapace and the main body of the *D. carinata* have separated, the animal became dead. Besides, this process also induced the eggs in the brood pouch and dropped into the culture medium and after that the larva started to swim in the medium. It can be conclude that the inorganic  $\text{Hg}^{2+}$  leads to exuviation and death. However, the main target organ of the *D. carinata* that causes its death ought to use the fluorescent microscope to detect.

The real mortality rate of the *D. carinata* in two different  $\text{Hg}^{2+}$  concentrations (5 and 10  $\mu\text{M}$ ) was not easy to detect, because it is difficult to determine whether the larva dropped from the brood chamber or they were already in the culture medium. However, it is easy to observe when the *D. carinata* start to die. Fig. 21 shows that the *D. carinata* started to die at 5  $\mu\text{M}$   $\text{Hg}^{2+}$  concentration from 60 minutes and at 10  $\mu\text{M}$   $\text{Hg}^{2+}$  concentration started to die at 50 minutes. The 100% estimated mortality rate was obtained at 3 hours and 2.5 hours in 5 and 10  $\mu\text{M}$   $\text{Hg}^{2+}$  concentrations respectively.

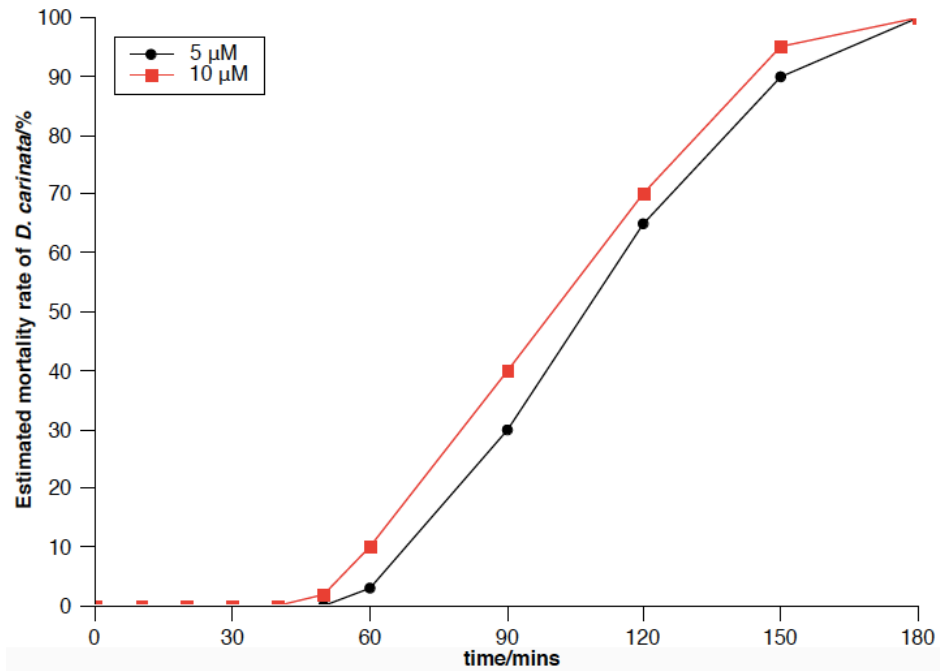


Fig. 21. Estimated death rate of *D. carinata* at 5 and 10 µM Hg<sup>2+</sup> concentration.

Furthermore, Hg<sup>2+</sup> concentration higher than 10 µM will cause the *D. carinata* to die too fast, therefore using >10 µM Hg<sup>2+</sup> was not suitable for checking the real bioaccumulation of *D. carinata* as the real value that the *D. carinata* can absorb Hg<sup>2+</sup> was not able to detect. Also, for the comparison with the algae protection capability, Jiang et al. (2016) observed that the abnormal rate of *E. gracilis* that incubated at a concentration higher than 10 µM Hg<sup>2+</sup> is relatively high. Hence Hg<sup>2+</sup> concentrations over 10 µM are not suitable to use in the following experiments. As for this, 5 and 10 µM Hg<sup>2+</sup> concentrations were used and 2.5 µM Hg<sup>2+</sup> concentration was applied additionally in the subsequent study.

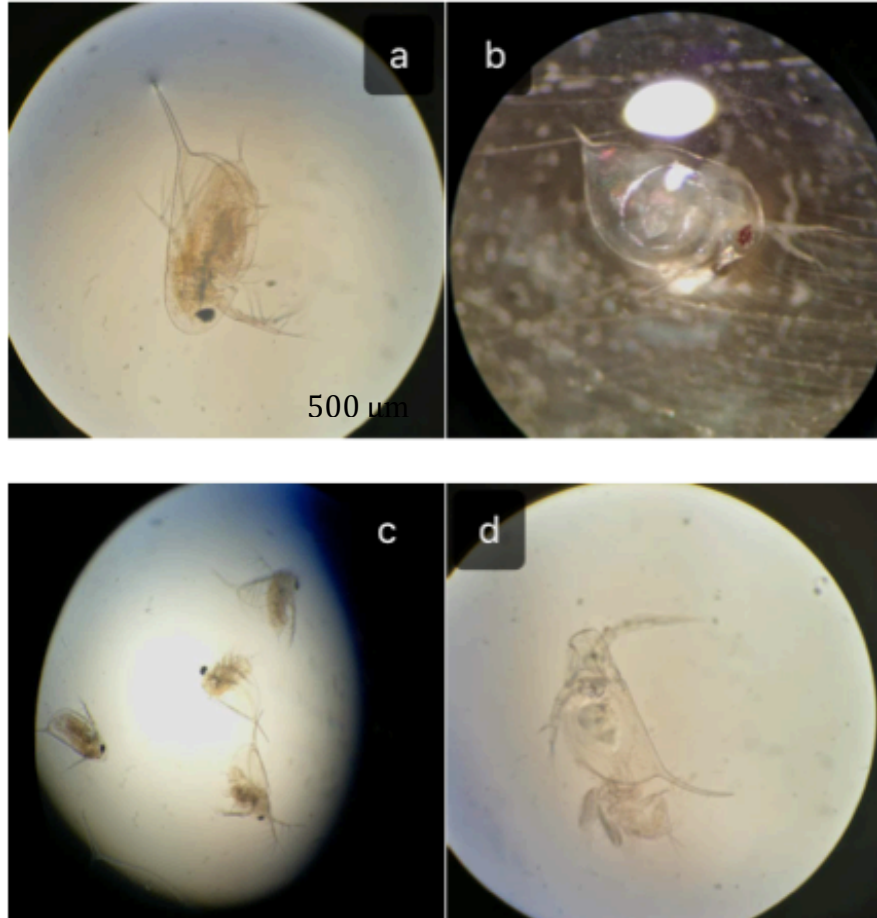


Fig. 22. (a) Started be toxic; (b) The deformation of carapace; (c) The carapace exuviated from the idiosoma and (d) The exuviated carapace.

### **5.3 AIEgen quantification for bioaccumulation of inorganic $\text{Hg}^{2+}$ in *D. carinata*.**

#### **5.3.1 Absorption of inorganic $\text{Hg}^{2+}$ in *D. carinata*.**

The *D. carinata* belongs to the order of Cladocera and has an open vascular system. Its protein coat is open rather than close. When eating, it moves the appendages and enables the food flow into the mouth with water stream. After entering the digest system, the food would transfer into the esophagus and move to the anus. In this process, the nutrition in the food can be

absorbed (Wei 1999). In this context, the diameter of the food or ion is smaller than the *D. carinata*'s mouth can be consumed. Different  $\text{Hg}^{2+}$  concentrations (2.5, 5 and 10  $\mu\text{M}$ ) are used for the direct absorption test.

Fig. 23 shows that there is a significant drop of  $\text{Hg}^{2+}$  in water at the beginning for all these three  $\text{Hg}^{2+}$  concentrations. This phenomenon indicates that the fast uptake of  $\text{Hg}^{2+}$  by the *D. carinata*. After 120 minutes, the  $\text{Hg}^{2+}$  in the water for these three groups of samples has plateaued. At the meantime, most of the *D. carinata* have died.

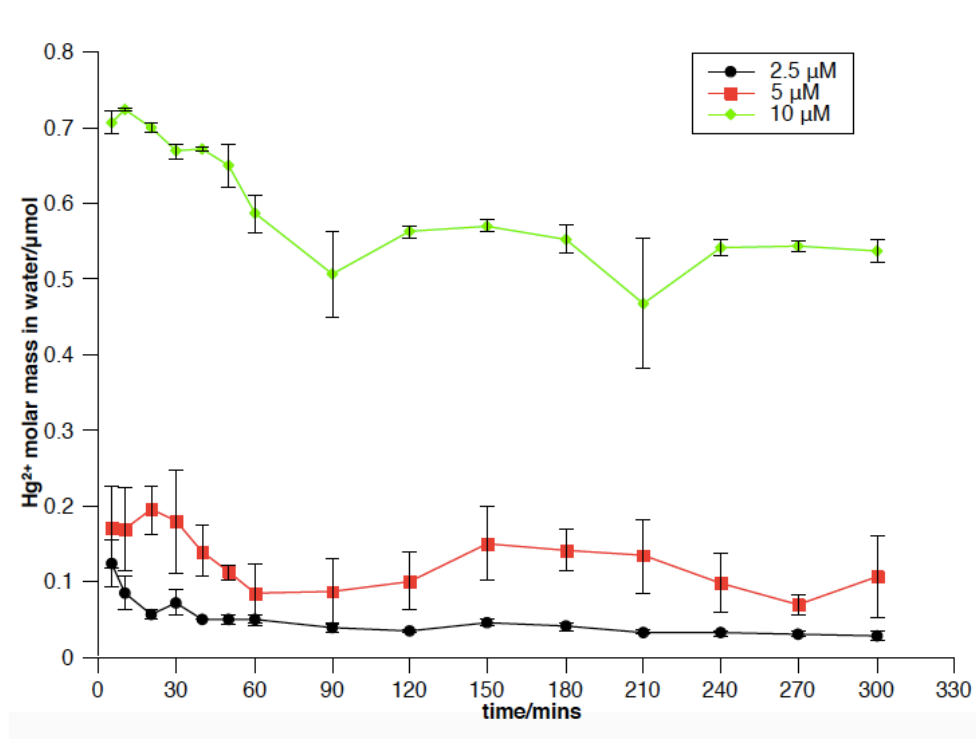


Fig. 23.  $\text{Hg}^{2+}$  in culture water over time (5, 10, 20, 30, 40, 50, 60, 90, 120, 150, 180, 210, 240, 270 and 300 minutes) of *D. carinata* cultivated in 2.5, 5 and 10  $\mu\text{M}$   $\text{Hg}^{2+}$ .

To confirm that the result is reliable through the AIE method, the ICP-MS method was used for determining  $\text{Hg}^{2+}$  concentration at 2.5  $\mu\text{M}$ , which is shown in Fig. 24. The ICP-MS result for  $\text{Hg}^{2+}$  concentration was slightly higher than that using the AIE method. It is because the organic carbon comes from the ACN can boost the growth and reproduction of the bacteria.

Those bacteria can significantly absorb  $\text{Hg}^{2+}$  as well. The relationship with bacteria and *D. carinata* in bioaccumulation needs further investigation (Jiang et al. 2016). However, the trend of both curves is similar.

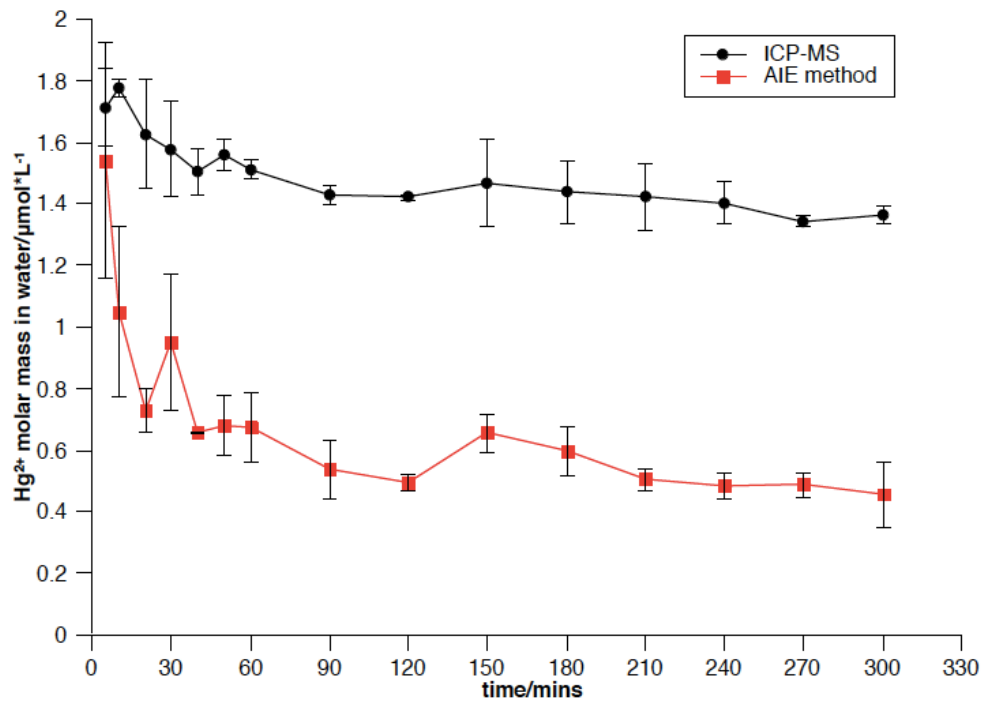


Fig. 24. Comparison of ICP-RMS and AIE method of culture medium  $\text{Hg}^{2+}$  concentration detection at 2.5  $\mu\text{M}$ .

### 5.3.2 Biorelease of inorganic $\text{Hg}^{2+}$ in *D. carinata*.

The biorelease of different  $\text{Hg}^{2+}$  concentration from bioaccumulated *D. carinata* was used to further explain the bioaccumulation of  $\text{Hg}^{2+}$  in *D. carinata*'s body. The period of 10 minutes was chosen as the absorption time of  $\text{Hg}^{2+}$  in *D. carinata*. This is because from the absorption test results (Fig. 23 and Fig. 24), when  $\text{Hg}^{2+}$  concentrations are 5  $\mu\text{M}$  and 10  $\mu\text{M}$  using the AIE method and is 2.5  $\mu\text{M}$  using the ICP-MS method, the absorption amount of  $\text{Hg}^{2+}$  in the water in all three tests climbed to a small peak and then decreased. Therefore, it might be an important factor for the *D. carinata* to release the pollutant inside their body. Besides, it can be sure that the *D.*

*carinata* were still alive, which means they were able to perform the biorelease process in the clean water. The *D. carinata* were transferred to the incubated container with Milli Q water. The molar of  $\text{Hg}^{2+}$  in the water with time changing is shown in Fig. 25. The *D. carinata* released a limited amount of  $\text{Hg}^{2+}$  to the clean water. The highest quantity is 0.025  $\mu\text{mol}$  at 2.5  $\mu\text{M}$  initial  $\text{Hg}^{2+}$  concentration and 0.018 and 0.005  $\mu\text{mol}$  at 5 and 10  $\mu\text{M}$  initial  $\text{Hg}^{2+}$  concentration respectively, which are really close to nil. This result can be ignored when calculated the bioaccumulation. Interestingly, the *D. carinata* turned up to death at 150 minutes and after 300 minute observation, all the *D. carinata* in the incubated container died. However, compared with the experimental groups, animals in the control without adding food and toxin were still alive. It is obvious that the *D. carinata* were less likely to release inorganic  $\text{Hg}^{2+}$  from their idiosoma if the  $\text{Hg}^{2+}$  concentration in the water is higher than 2.5  $\mu\text{M}$ . It can be confirmed that the *D. carinata* have accumulated the inorganic  $\text{Hg}^{2+}$  in the target organs in their body.

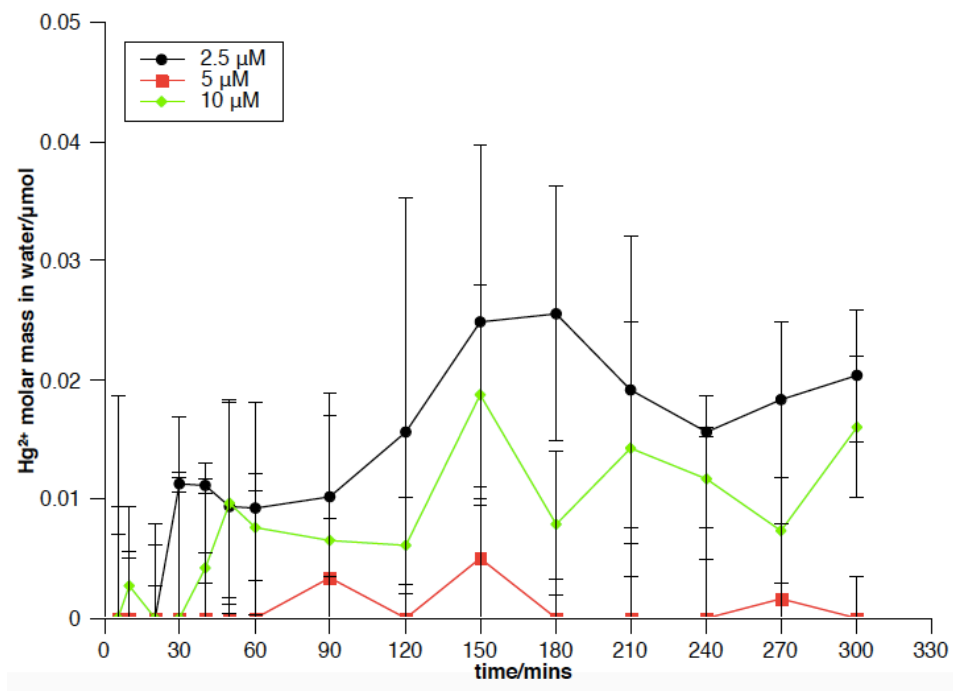


Fig.25 Biorelease of *D. carinata* at three different  $\text{Hg}^{2+}$  concentrations.

### 5.3.3 The bioaccumulation of different inorganic $\text{Hg}^{2+}$ concentrations in *D. carinata*.

It can be concluded that the  $\text{Hg}^{2+}$  accumulated in the *D. carinata*'s body is that they have absorbed. The molar of bioaccumulation ( $A_t$ ), bioaccumulation efficiency ( $E_t$ ) and bioaccumulation ratio ( $R_t$ ) of inorganic  $\text{Hg}^{2+}$  in *D. carinata* were calculated as

$$A_t = C_0 \times V_0 - m_w$$

where  $A_t$  is the molar of  $\text{Hg}^{2+}$  bioaccumulated in *D. carinata* at time  $t$ ;  $C_0$  is the initial concentration of  $\text{Hg}^{2+}$  added in incubated medium;  $V_0$  is the volume of incubated medium;  $m_w$  is the remaining molar of  $\text{Hg}^{2+}$  in the culture medium (water) at time  $t$ .

$$E_t = A_t/t$$

where  $E_t$  is the bioaccumulation efficiency of  $\text{Hg}^{2+}$  in *D. carinata* at time  $t$ ;  $t$  is the time for  $\text{Hg}^{2+}$  absorption in *D. carinata* (Jiang et al. 2016).

$$R_t = m_t/m_m = m_t/(m_0 - m_t)$$

where  $R_t$  is the bioaccumulation ratio of  $\text{Hg}^{2+}$  in *D. carinata* at time  $t$ ;  $m_m$  is the molar of  $\text{Hg}^{2+}$  in the culture medium (water) at time  $t$ ;  $m_t$  is the molar of  $\text{Hg}^{2+}$  absorbed by the *D. carinata* at time  $t$ ;  $m_0$  is the initial molar of  $\text{Hg}^{2+}$  added in incubated medium with  $m_0 = m_t + m_m$  (Jiang et al. 2016).

The bioaccumulation of  $\text{Hg}^{2+}$  in *D. carinata* is indicated in Fig. 26. When the concentration of  $\text{Hg}^{2+}$  is 2.5  $\mu\text{M}$  and 5  $\mu\text{M}$  initially in the culture medium, the bioaccumulation depends on time and  $\text{Hg}^{2+}$  concentration. In the 10  $\mu\text{M}$   $\text{Hg}^{2+}$ , the bioaccumulation is less than that of 5  $\mu\text{M}$  initial  $\text{Hg}^{2+}$  concentration in culture medium. The reason for it can be due to the velocity of *D. carinata*'s



death that is faster than that in 5  $\mu\text{M}$ . When the *D. carinata* begins to die, the absorption of  $\text{Hg}^{2+}$  reduces, which causes the final bioaccumulation of  $\text{Hg}^{2+}$  in the culture medium started at 10  $\mu\text{M}$  less than that at 5  $\mu\text{M}$ . The bioaccumulation efficiency is demonstrated in Fig. 27. In the first five minutes, the culture medium with initial  $\text{Hg}^{2+}$  concentration at 5  $\mu\text{M}$  had the highest bioaccumulation efficiency, whereas the highest  $\text{Hg}^{2+}$  concentration, which is 10  $\mu\text{M}$ , did not correspond to the highest bioaccumulation efficiency. After 30 minutes, all these three concentrations of  $\text{Hg}^{2+}$  presented a similar trend of bioaccumulation efficiency with time. From 5 to 30 minutes, all of the bioaccumulation efficiencies decreased significantly to a lower value, especially for the  $\text{Hg}^{2+}$  concentration at 5  $\mu\text{M}$ , because most *D. carinata* were still alive. After 150 minutes, three bioaccumulation efficiency curves became relatively stable and stayed near the zero value. This is because nearly all the *D. carinata* have already died and they were not able to absorb more inorganic  $\text{Hg}^{2+}$  to their idiosoma. The bioaccumulation ratio in each initial  $\text{Hg}^{2+}$  concentration is shown in Fig. 28. It demonstrates that in 5 hours, the  $\text{Hg}^{2+}$  bioaccumulation ratio has nearly reached 6 at 2.5  $\mu\text{M}$  and exceeded 2.5 and 0.24 at 5 and 10  $\mu\text{M}$  respectively. This shows that the highest bioaccumulation amount of  $\text{Hg}^{2+}$  in *D. carinata* was at 2.5  $\mu\text{M}$ , and which has the lowest damage to the *D. carinata*. This phenomenon also confirmed that the initial 10  $\mu\text{M}$   $\text{Hg}^{2+}$  concentration in the culture medium could more likely cause the death of *D. carinata* depending on the time period. Similar testing concentration of inorganic  $\text{Hg}^{2+}$  in the *Daphnia*, which enables the *D. carinata* remain alive, was also reported (Tsui & Wang 2004). The range of testing concentration of inorganic  $\text{Hg}^{2+}$  was 0.28 to 28.0  $\mu\text{g/litter}$ , which is equivalent to the molar concentration of 0.00103  $\mu\text{M}$  to 0.103  $\mu\text{M}$  (the molar mass of  $\text{HgCl}_2$  is 271.49 g/mol). This testing concentration of inorganic  $\text{Hg}^{2+}$  enables the *Daphnia* to live about 8 hours. It is obvious that the molar concentrations that were used in the thesis

experiment were relatively high. Hence, it is not surprised that the *D. carinata* cannot live more than three hours.

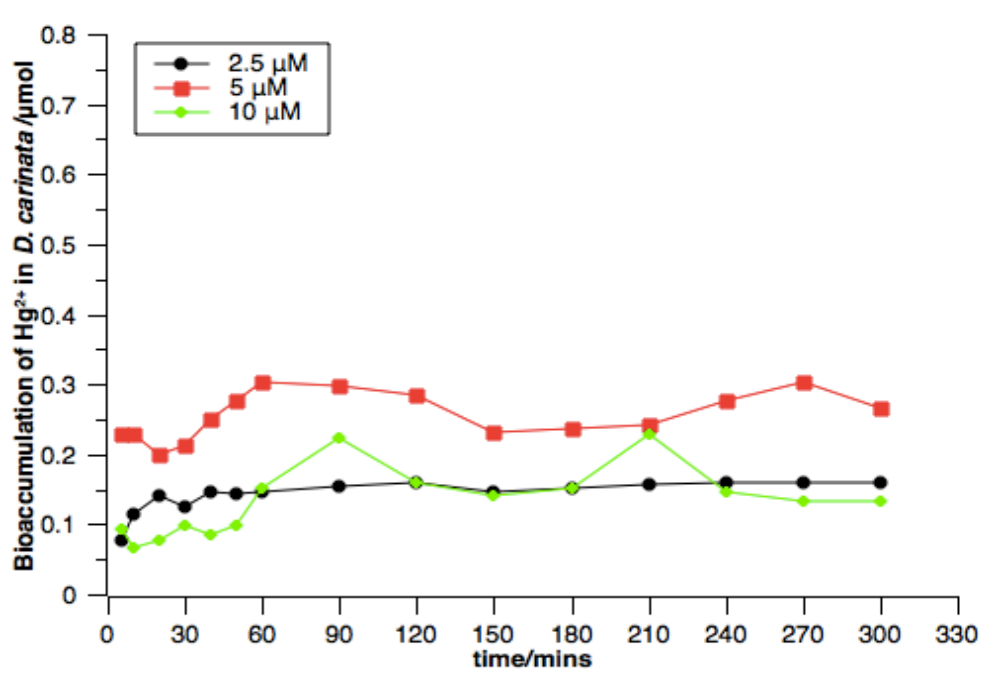


Fig. 26. Bioaccumulation of *D. carinata* in three different Hg<sup>2+</sup> initial concentrations.

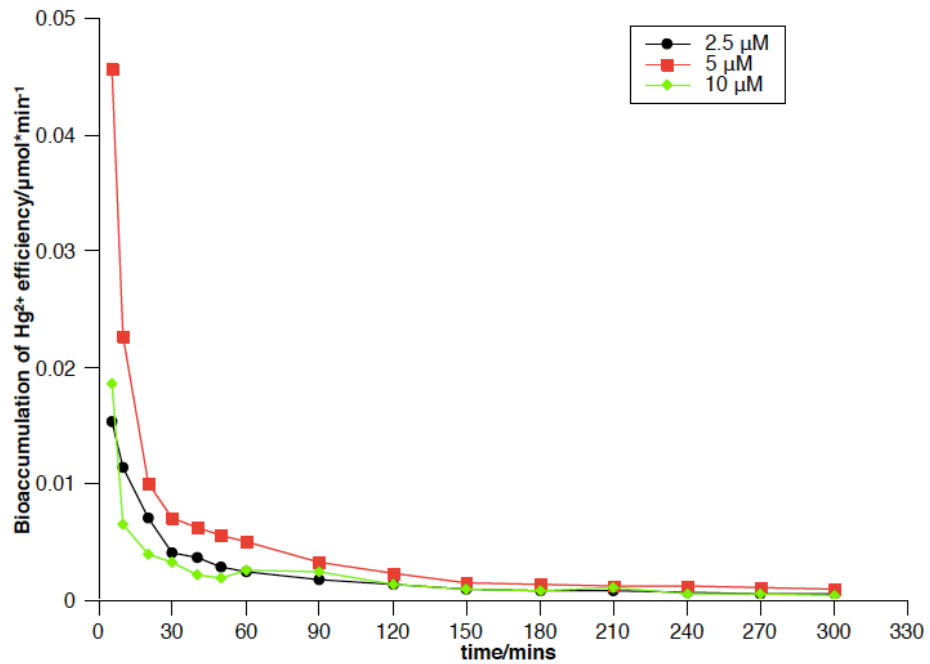


Fig. 27. Bioaccumulation efficiency of *D. carinata* in three different  $\text{Hg}^{2+}$  initial concentrations.

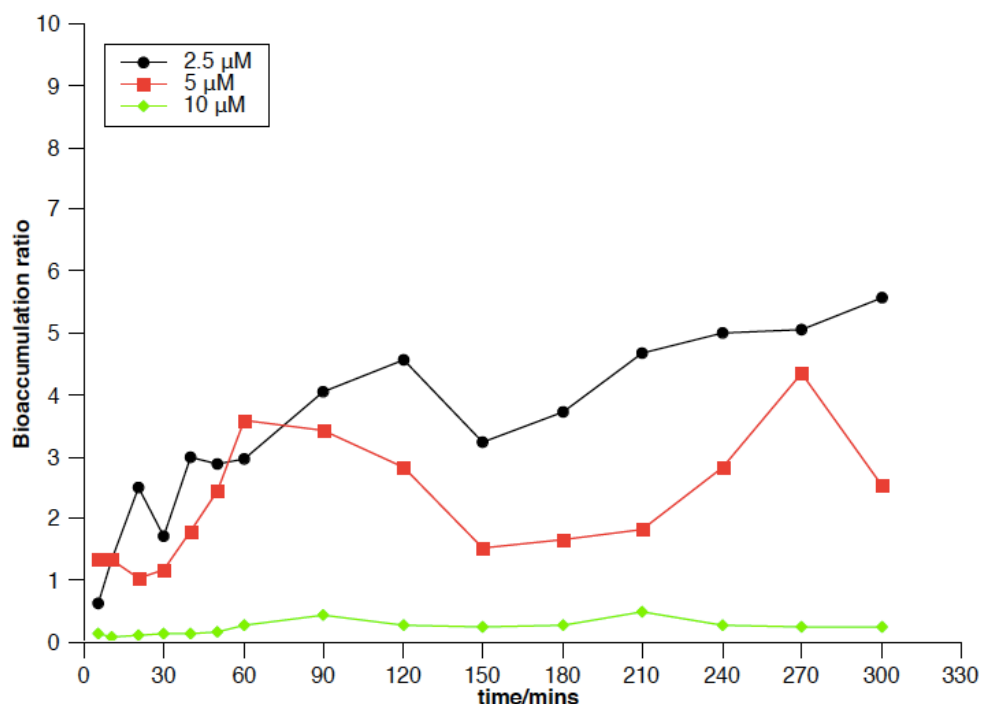


Fig. 28. Bioaccumulation ratio of in three different  $\text{Hg}^{2+}$  initial concentrations.

#### 5.4 In vivo visualization of $\text{Hg}^{2+}$ dynamics within *D. carinata* by AIEgen under fluorescence microscope.

The m-TPE-RNS has been published to determine inorganic  $\text{Hg}^{2+}$  in living cells. As for this, it is encouraged that the potential  $\text{Hg}^{2+}$  sensing performance through m-TPE-RNS in the solution state can apply for evaluating the  $\text{Hg}^{2+}$  in the living *D. carinata*. This can be achieved by imaging. The sample in Fig. 29 (a) is in the control group for the AIE method. Without the interaction of AIEgens and inorganic  $\text{Hg}^{2+}$ , the image is not able to show any fluorescent signals. Similarly, when the live *D. carinata* were only polluted by inorganic  $\text{Hg}^{2+}$  without AIEgens, non-fluorescent signal

from the image can be obtained (Fig. 29 (b)). From Fig. 29 (c), when the *D. carinata* incubated with m-TPE-RNS, the blue fluorescent signal showed. This blue fluorescent signal was located in the wavelength between 460 to 550 nm. When the *D. carinata* have been exposed to inorganic  $\text{Hg}^{2+}$  first and then were pigmented by m-TPE-RNS, the red fluorescent signal showed in the image and this red signal was located in the wavelength between 570 to 610 nm (Fig. 29 (d)). The relative body structure and anatomy of daphnia can be obtained in Fig. 15.

After being exposed in the culture medium for 5 minutes and then pigmented by AIEgens, the weak emission signal in red colour was observed both at the compound eyes and the carapace. (Fig. 30 (a)). This phenomenon demonstrated that these two organs in the *D. carinata* were the initial targets for the inorganic  $\text{Hg}^{2+}$ . From Fig. 30 (b), when the exposure time increased, the emission signal in red colour became more evident in the compound eyes. Interestingly, in the testing period, there was no any fluorescent signal available from the ocellus as well as the brain, even though these two organs were close to the compound eyes (Fig. 31). In addition, the carapace performed the similar trend. When the exposure time increased, the strong red colour signal was obtained (Fig. 32).

When the experiment process continued to expose the *D. carinata* to the inorganic  $\text{Hg}^{2+}$  for 20 minutes, the red fluorescent emission signal was able to detect at the anterior body parts as well as embryos (Fig. 30 (b)). When it continued to 60 minutes, at the posterior intestine and shell gland, the kidney of *D. carinata*, can also obtain the red fluorescent signal emission (Figs. 30 (c) and 30 (d)). The previous study (Kasper et al. 2009) showed that different fish tissues, such as muscles, kidneys, gonads, livers and guts, are the targets of intake  $\text{Hg}^{2+}$ , no matter for the inorganic one or the organic one. Korbas et al. (2012) also showed that in the brains, olfactory epitheliums, eyes, guts and kidneys could find the trace of  $\text{Hg}^{2+}$  in zebrafish larvae while could

hardly find any in the heart. However, many studies did not cover the area of zooplankton. Using the AIE method can easily achieve and detect the dynamic of inorganic  $\text{Hg}^{2+}$  in the *D. carinata*. Figs. 30 (e) and 30 (f) show that the red fluorescent emission signals were not able to obtain from the ocellus, brain and heart of the *D. carinata*. In conclusion, the compound eyes, carapace, embryos, intestine and the shell gland would be the target organs of inorganic  $\text{Hg}^{2+}$  to *D. carinata*. However, the ocellus, brain and the heart of the *D. carinata* were not targeted. It can be also concluded that the reason that cause the *D. carinata* death could be the damage to the compound eyes and the major one can be the exuviation of the carapace from the idiosoma.

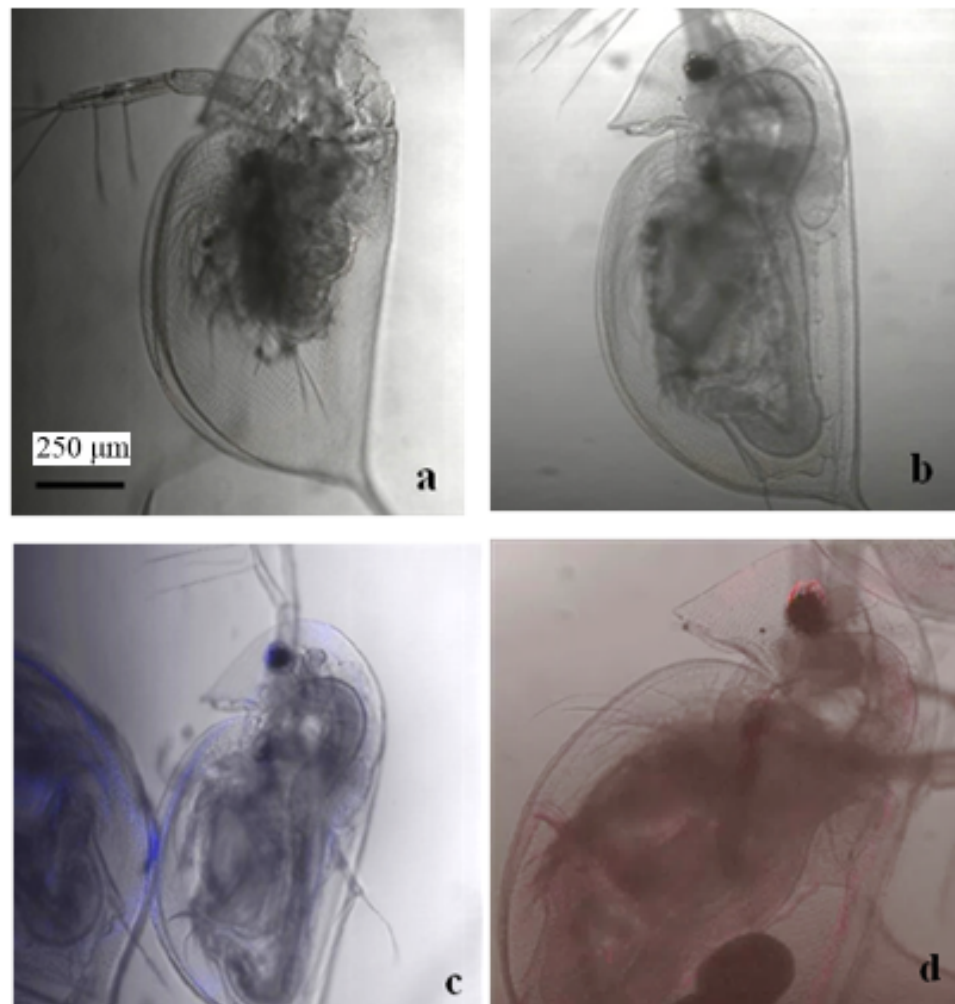


Fig. 29. Confocal microscope images of *D. carinata*. (a) Without inorganic  $\text{Hg}^{2+}$  polluted of *D. carinata* and AIEgens staining (b) *D. carinata* polluted

by inorganic  $\text{Hg}^{2+}$ , without interaction of AIEgens (c) *D. carinata* interact with AIEgens without combining with  $\text{Hg}^{2+}$  and (d) *D. carinata* cultivated in  $\text{Hg}^{2+}$  solution with pigment with AIEgens.

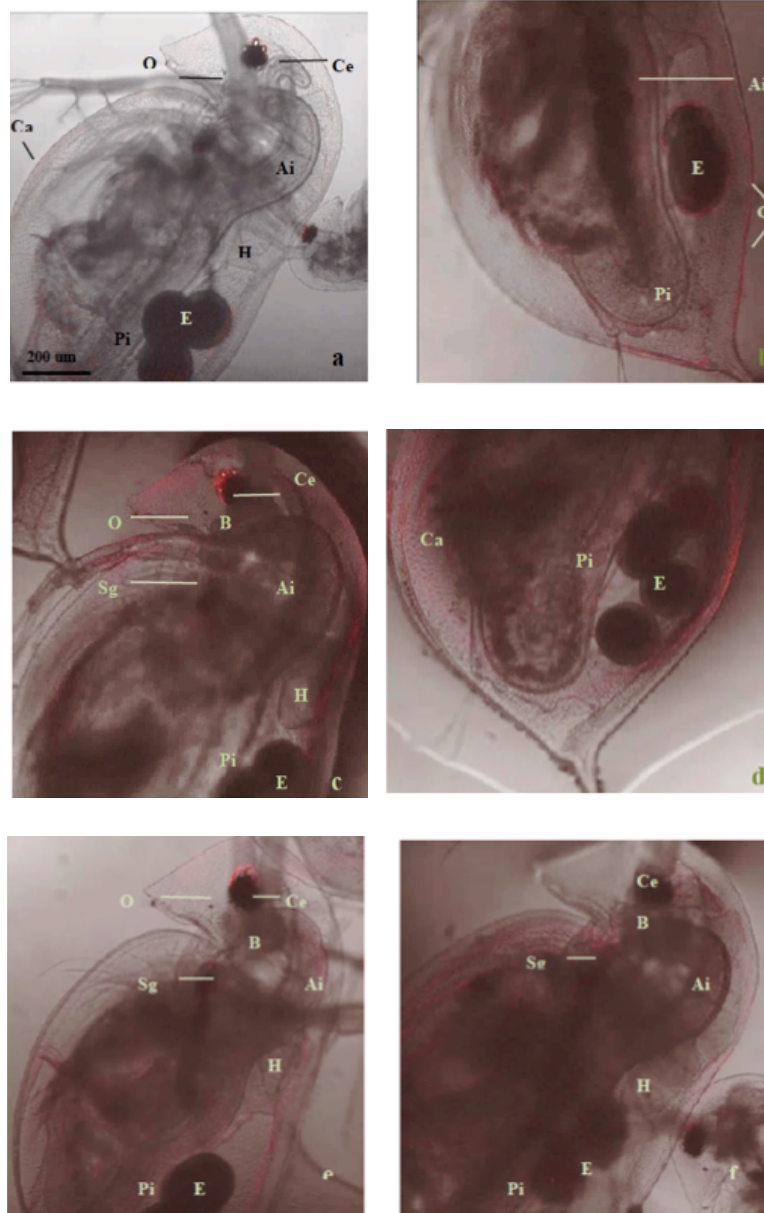


Fig. 30. Confocal fluorescent images of *D. carinata* incubated with inorganic  $\text{Hg}^{2+}$  for (a) 5 minutes; (b) 20 minutes; (c&d) 60 minutes; (d) 120 minutes; and (e) 150 minutes. Ai: anterior intestine; B: brain; Ca: carapace; Ce: compound eye; E: embryo; H: heart; O: ocellus Pi: posterior intestine; Sg: shell gland.

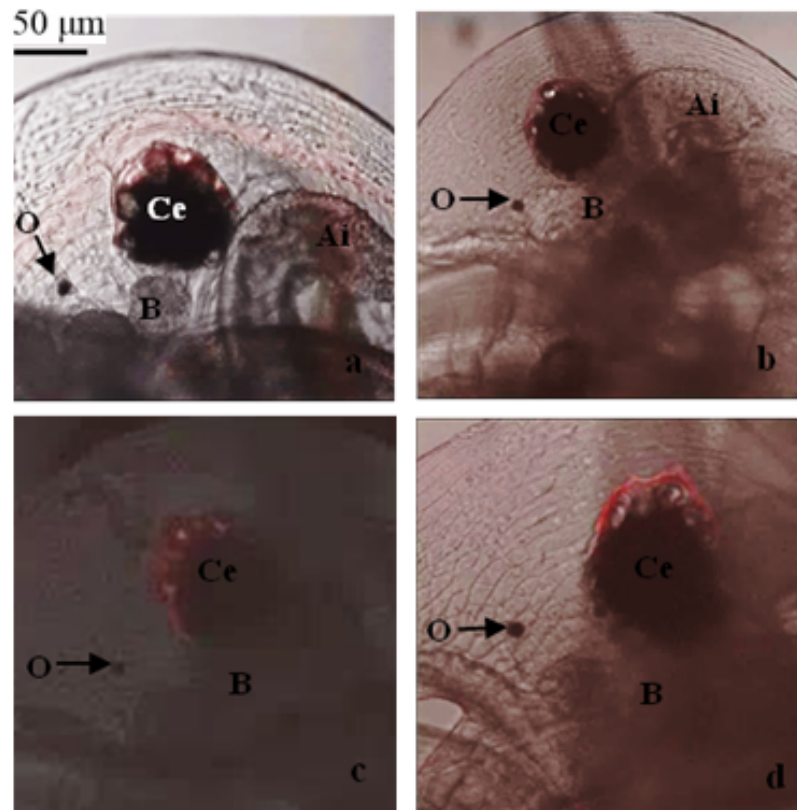


Fig.31 Red signal emission in fluorescent images of compound eyes in *D. carinata* incubated with  $\text{Hg}^{2+}$  for (a) 5 minutes; (b) 10 minutes; (c) 60 minutes; and (d) 120 minutes. Ai: anterior intestine; B: brain; Ce: compound eye; O: ocellus.

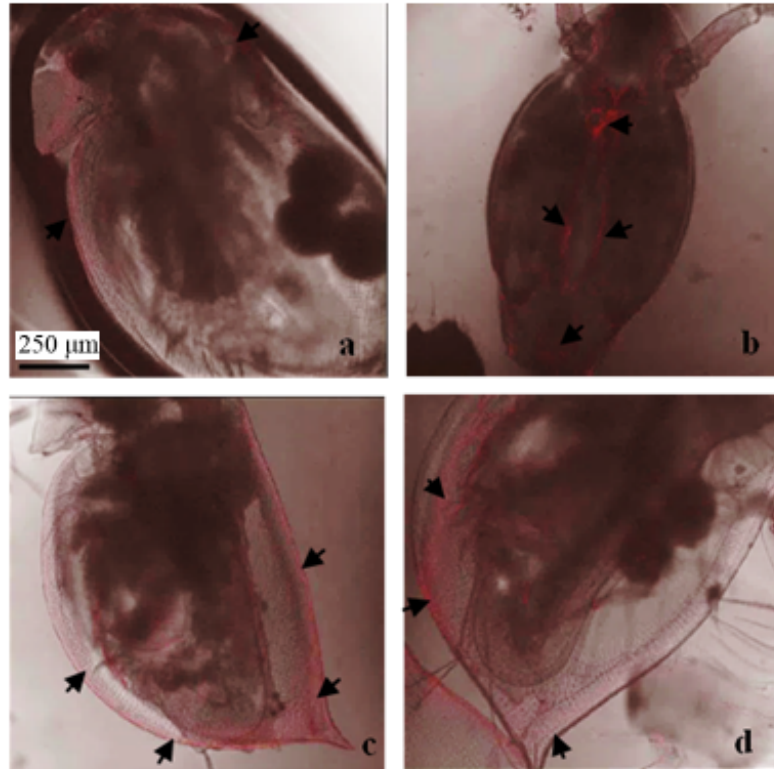


Fig.32 Red signal emission in fluorescent images of carapace in *D. carinata* incubated with Hg<sup>2+</sup> after (a) 30 minutes; (b) 60 minutes; (c) 90 minutes; and (d) 150 minutes. The arrows indicate red fluorescence (Hg<sup>2+</sup>).

### 5.5 The response of *Daphnia carinata* to toxic Hg<sup>2+</sup> enriched *Euglena gracilis*.

In the natural environment, the bioaccumulation process of contaminants not only comes from direct absorption but also from the food that the *D. carinata* consume. In order to compare the different bioaccumulation processes of Hg<sup>2+</sup> from the lower level producers and from direct absorption, different Hg<sup>2+</sup> concentrations of *E. gracilis* (a species of microalgae) was applied for determination. The 50% lethal and various Hg<sup>2+</sup> concentrations of the *E. gracilis* was 20 μM confirmed by Jiang et al. (2016). Therefore, 5 μM and 10 μM Hg<sup>2+</sup> concentrations were applied in this study. The density of the *E. gracilis* was observed under the optical microscope with a camera by using a



haemocytometer. Nine small squares in the count block were selected randomly (Fig. 33). The bioaccumulation process of *E. gracilis* would turn to a stable level after absorbing the  $\text{Hg}^{2+}$  for 30 minutes (Jiang et al. 2016), and this time was applied to finish the pollution of the *E. gracilis* with different  $\text{Hg}^{2+}$  concentrations. The supernatant from the culture containers was used to determine the quantity of  $\text{Hg}^{2+}$  left in the culture medium. Normally, it takes 20 to 30 minutes for the *D. carinata* to uptake most of the *E. gracilis* in the culture medium. Hence, every 30 minutes, the live *D. carinata* were taken out to observe under the optical microscope until 3.5 hours. The response of the *D. carinata* incubated in 5  $\mu\text{M}$  and 10  $\mu\text{M}$   $\text{Hg}^{2+}$  from 20 minutes to 3 hours was recorded by images and videos under optical microscope (Figs .34 and 35). When the *D. carinata* consumed the *E. gracilis* into their digestive system, their intestinal canal turned into green. After the *D. carinata* have digested the *E. gracilis*, the intestinal canal turned back to transparency (Fig .37). Figs. 34 and 35 shows that after consuming for 20 minutes, the *E. gracilis* contaminated by different  $\text{Hg}^{2+}$  concentrations were nearly consumed by the *D. carinata*. In addition, it is surprised that after consuming the polluted *E. gracilis*, the starting death time for the *D. carinata* increased to 90 minutes for both  $\text{Hg}^{2+}$  polluted concentration in *E. gracilis*. Until reaching 3.5 hours, which was the finishing time for the experiment, there was still a little amount of living *D. carinata*. Fig. 36 shows that the *D. carinata* began to die at 90 minutes in both  $\text{Hg}^{2+}$  concentration contaminated by the *E. gracilis*. The mortality rates have not reached to 100% until 3.5 hours. Compared to that without feeding *E. gracilis* to *D. carinata*, a higher survival rate within 3 hours was obtained. It is certainly that *E. gracilis* indeed has the protection effect to *D. carinata*. The further test of 12 hours observation continued to detect whether these survived *D. carinata* can still live to the end, in the meantime the living *D. carinata* were transferred to the culture container containing Milli Q water and fed by bakery yeast. The

remaining culture medium after testing 3.5 hours for the *D. carinata* was collected for the detection of the remaining  $\text{Hg}^{2+}$ . During 3.5 hours, there was small amount of  $\text{Hg}^{2+}$  in the culture medium (Fig. 38). It can be deduced that the *D. carinata* digested the *E. gracilis* and then excreted to the outside of the bodies through their digestive system. These shielded  $\text{Hg}^{2+}$  ions were released through digestion. This is the lethal reason for the most *D. carinata* within 3.5 hours. After being transferred to the Milli Q water and incubated for 12 hours with feeding baker's yeast, all the survival *D. carinata* were dead. The reason can be due to low biorelease. Most of the survival *D. carinata* should bioaccumulate the  $\text{Hg}^{2+}$  in the culture medium, but during that time they still alive. Even though they were transferred to the Milli Q water for further cultivation, the  $\text{Hg}^{2+}$  remaining in their bodies could not be released.



Fig. 33. *E. gracilis* cells observation under optical microscope. The arrow indicates the *E. gracilis* cells.

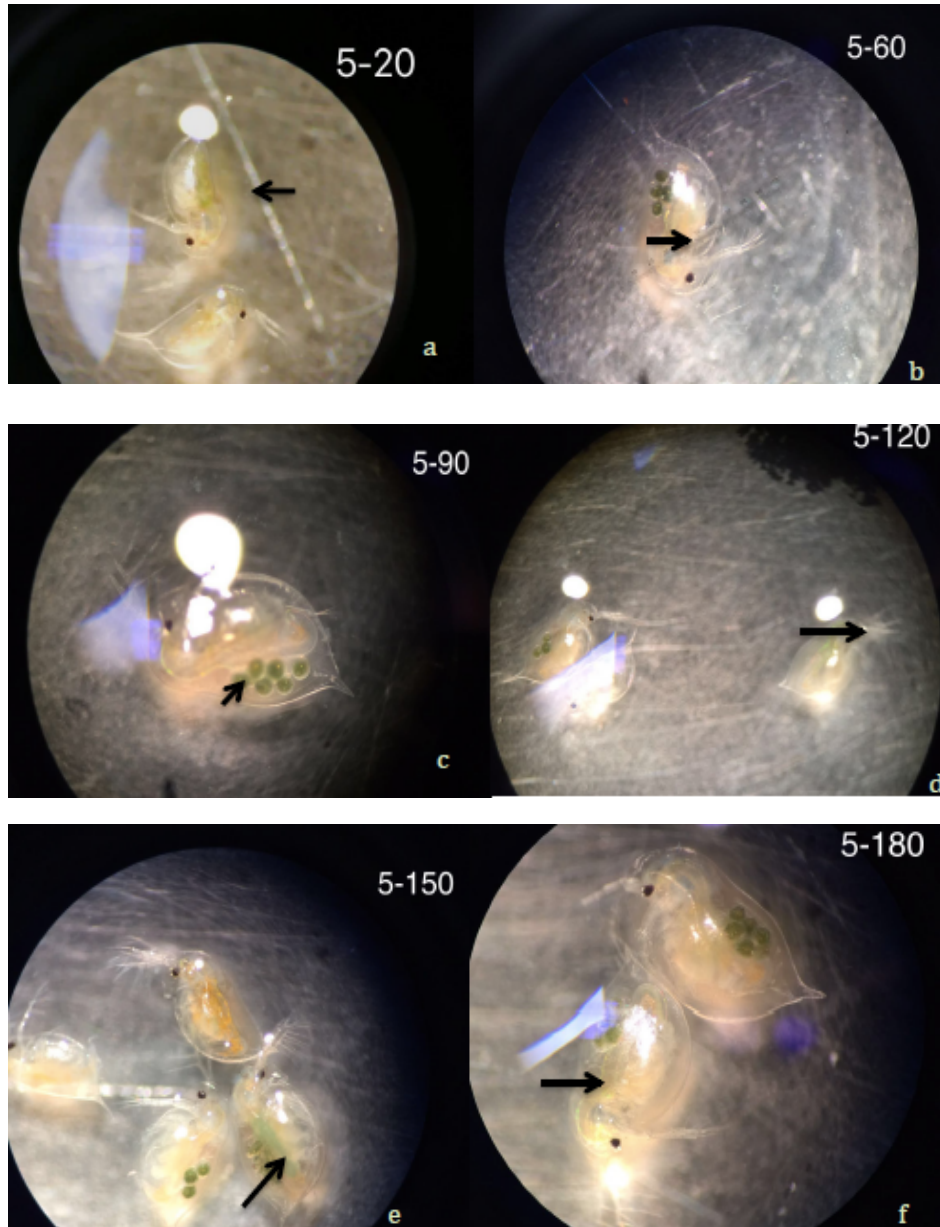


Fig. 34. The *E. gracilis* contaminated by 5  $\mu\text{M}$   $\text{Hg}^{2+}$  and fed to the *D. carinata*. (a) *D. carinata* absorbed after 20 minutes (b) 60 minutes (c) 90 minutes (d) 120 minutes (e) 150 minutes and (f) 180 minutes. The black arrow indicates the intestinal canal.

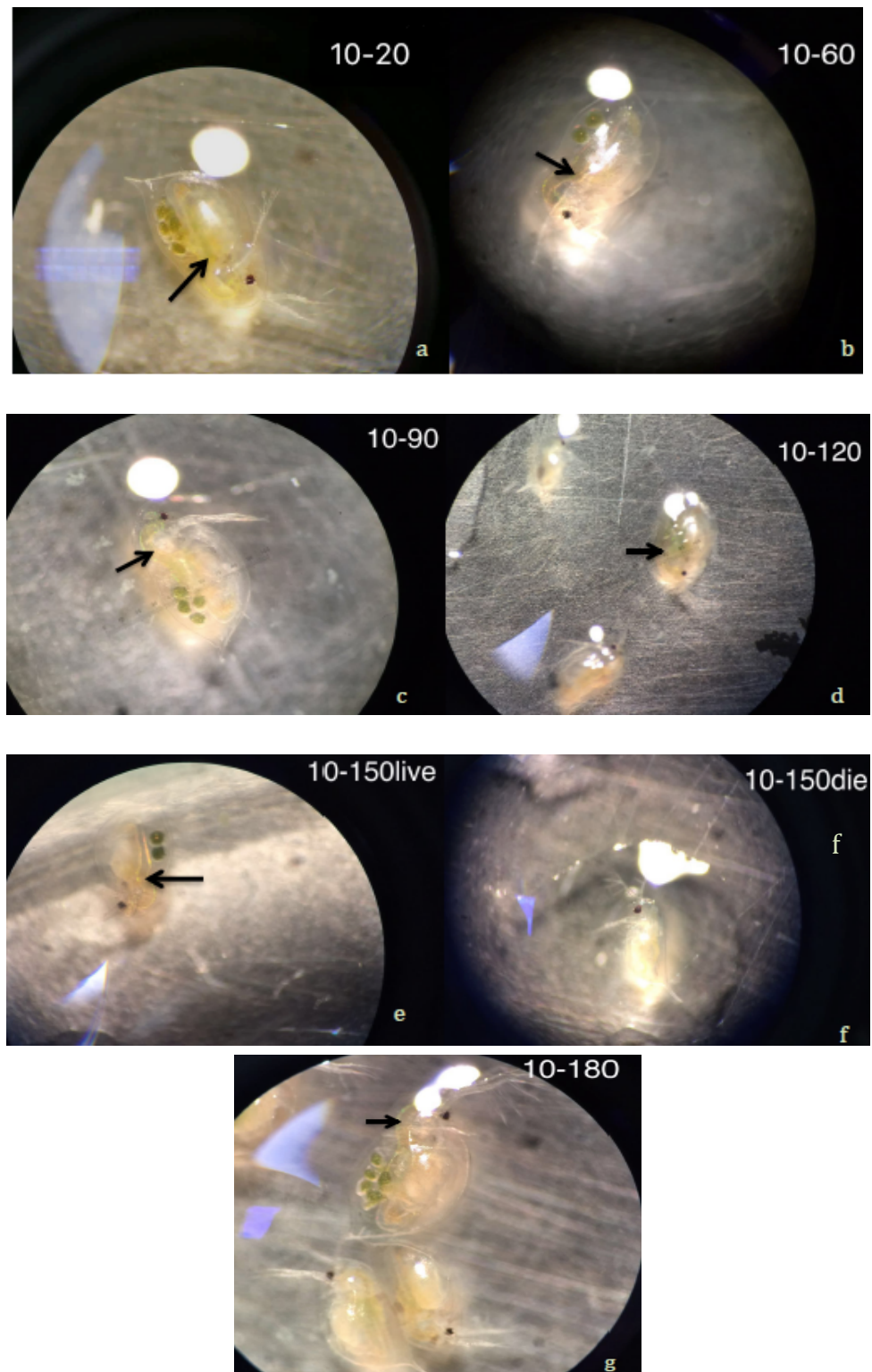


Fig. 35. The *E. gracilis* contaminated by  $10 \mu\text{M Hg}^{2+}$  and fed to the *D. carinata*. (a) *D. carinata* absorbed after 20 minutes (b) 60 minutes (c) 90 minutes (d) 120 minutes (e) 150 minutes still alive (f) 150 minutes already dead and (g) 180 minutes. The black arrow indicates the intestinal canal.

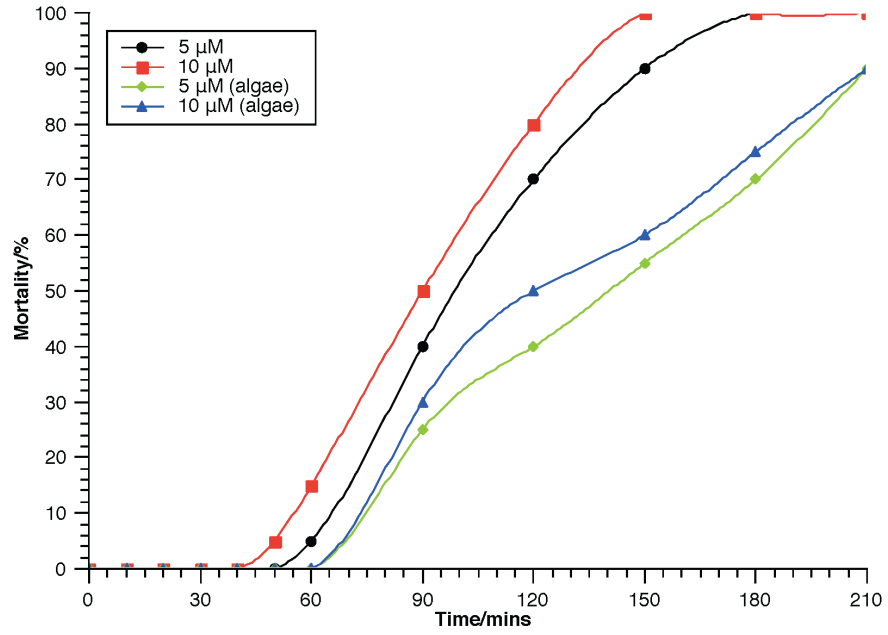


Fig. 36. Estimated mortality rates in direct absorption and along food chain.

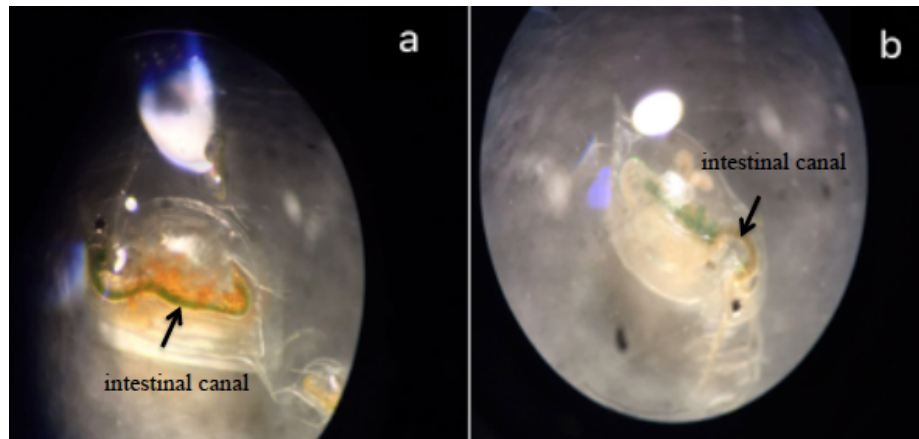


Fig. 37, (a) The *E. gracilis* in the intestinal canal of *D. carinata* and (b) digested from the intestinal canal of *D. carinata*.

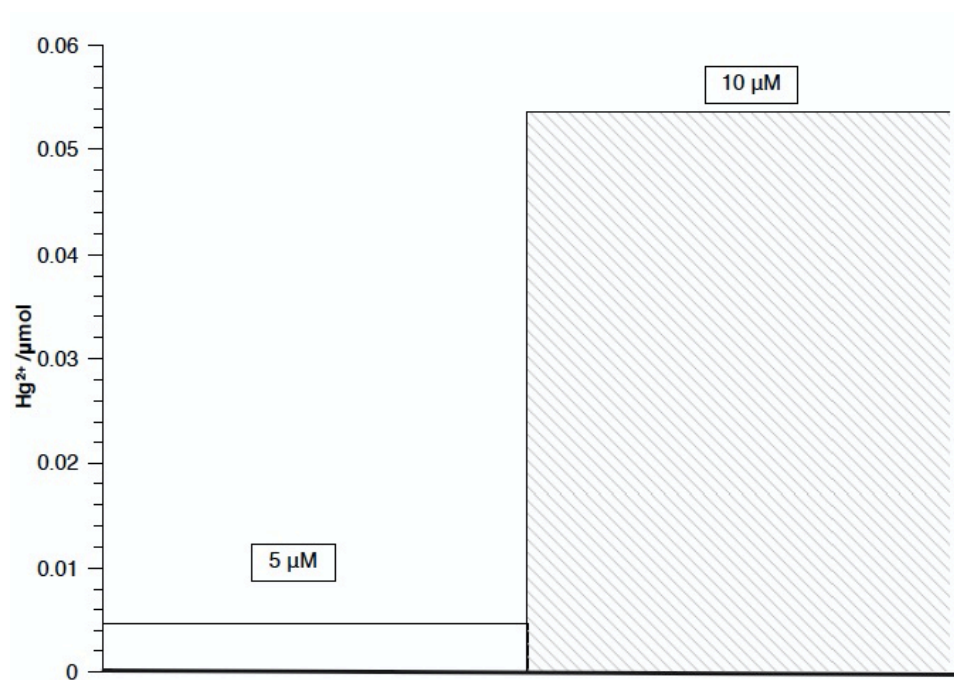


Fig. 38. The start and final  $\text{Hg}^{2+}$  concentrations remain in the *D. carinata* culture medium.

## 6. Conclusion

In this study, a novel, sufficient and effective AIE method was demonstrated. The inorganic  $\text{Hg}^{2+}$  bioaccumulated in zooplankton was clearly quantified by the specific AIEgen, i.e., m-TPE-RNS. The bioaccumulation process of inorganic  $\text{Hg}^{2+}$  in *D. carinata* can be determined by the AIE method. By detecting and confirming the fluorescence ratio, the  $\text{Hg}^{2+}$  concentration in the culture medium can be calculated with the standard curve. Furthermore, through knowing the  $\text{Hg}^{2+}$  concentration in the culture medium, the bioaccumulation and biorelease quantity of  $\text{Hg}^{2+}$  in *D. carinata* can be deduced as well. Besides, the dynamic of  $\text{Hg}^{2+}$  in the *D. carinata* was able to be observed under the fluorescent microscope, which is a straightforward method to know the cause of the *D. carinata*'s death. This novel AIE method provides an effective and visualized way to determine the inorganic  $\text{Hg}^{2+}$  bioaccumulated in the aquatic organisms.

## 7. Acknowledgements

This thesis was supported by College of Science and Engineering Flinders University. Associate Professor Youhong Tang and Professor Jianguang Qin from Flinders University were grateful for the support of the experiment reagents, materials, experimental instruments and experimental sites. Dr. Tao He from South West University in China was grateful for the support of the guidance of technical operations.

## 8. References

- Allibone J., Fatemian E., Walker P. (1998) Determination of mercury in potable water by ICP-MS using gold as a stabilising agent, *Journal of Analytical Atomic Spectrometry*, vol. 14, pp. 235-239.
- Bao Z., Shang L., Feng X., Meng B. (2013) Applications of isotopic labeling technique in the studies of mercury biogeochemistry. *Chinese Journal of Ecology*, vol. 32, no. 5, pp. 1335-1346.
- Beijing X&D Shuaiyi Technology CO., LTD (2012) Atomizer. *Beijing X&D Shuaiyi Technology CO., LTD*, viewed 14 June 2017, [http://www.xiandasy.com/mod\\_article-article\\_content-article\\_id-302.html](http://www.xiandasy.com/mod_article-article_content-article_id-302.html).
- Bryan G. W., Waldichuk M., Pentreath R. J., and Darracott Ann (1979) Bioaccumulation of marine pollutants, *Philosophical Transactions of the Royal Society of London. Series B, Biological Sciences*, vol. 286, no. 1015, pp. 483-505.
- Chen H., Cao S., Zeng X, (2000) Application of inductively coupled plasma mass spectrometry in biological samples analysis. *Chinese Journal of Analytical Chemistry*, vol. 29, no 5, pp. 592-600.

- Chen Y., Zhang W., Cai Y., Kwok R. T. K., Hu Y., Lam J. W. Y., Gu X., He Z., Zhao Z., Zheng X., Chen B., Gui C., Tang B. (2017) AIEgens for dark through-bond energy transfer: design, synthesis, theoretical study and application in ratiometric Hg<sup>2+</sup> sensing. *Chemical Science*, vol. 8, pp. 2047-2055.
- Chiou C., Jiang S., Danadurai K. S. K. (2001) Determination of mercury compounds in fish by microwave-assisted extraction and liquid chromatography-vapor generation-inductively coupled plasma mass spectrometry, *Spectrochimica Acta Part B*, vol. 56, pp. 1133-1142.
- Clarkon T. W. (1998) Human toxicology of mercury. *The Journal of Trace Elements in Experimental Medicine*, vol. 11, no. 1 pp. 303-317.
- Deshpande K., Mishra R. K., Bhand S. (2010) A high sensitivity micro format chemiluminescence enzyme inhibition assay for determination of Hg(II). *Sensors*, vol. 10, no. 7, pp. 6377-6394.
- Ding D., Li K., Tang B. (2013) Bioprobes based on AIE fluorogens. *Accounts of Chemical Research*, vol. 46, no. 11, pp.2441-2453.
- Ebert D. (2005). Introduction to daphnia biology, in *Ecology, Epidemiology, and Evolution of Parasitism in Daphnia*, Bethesda (MD): National Center for Biotechnology Information, US.
- Fox D.L. (1972) Chitin-bound keto-carotenoids in a crustacean carapace, *Comparative Biochemistry and Physiology Part B: Comparative Biochemistry*, vol. 44, no. 4, pp. 953-962.
- Gliwicz Z M. (2008). Zooplankton in Patrick O *Limnology and Limnetic Ecology*, pp. 461–516.
- Guo F., Gai W., Hong Y., Tang B., Qin J., Tang Y. (2015) Aggregation-induced emission fluorogens as biomarkers to assess the



viability of microalgae in aquatic ecosystems. *Royal Society of Chemistry*, vol. 51, pp. 17257-17260.

- Gobas F., de Wolf W., Burkhard L. P., Verbruggen E., Plotzke K. (2009) Revising bioaccumulation criteria for POPs and PBT *Integrated Environmental Assessment and Management*, vol. 5, pp. 624-637.
- Gupta V. K., Ganjali M. R., Norouzi P., Khani H., Nayak A., Agarwall S. (2011) Electrochemical analysis of some toxic metals by ion-selective electrodes. *Critical Reviews in Analytical Chemistry*, vol. 41, pp. 282-313.
- Hebert P (2005) Functional genomics thickens the biological plot, *PLoS Biology*, vol. 3, no. 6. doi: 10.1371/journal.pbio.0030219
- Hong Y., Lam J. W. Y., Tang B. (2009) Aggregation-induced emission: phenomenon, mechanism and applications. *Royal Society of Chemistry*, pp. 4332-4353.
- Korbas M., Macdonald T. C., Pickering I. J., George G. N., Krone P. H. (2012) Chemical form matters: differential accumulation of mercury following inorganic and organic mercury exposures in zebrafish larvae. *ACS Chemical Biology*, vol. 7, no. 2, pp. 411-20.
- Jiang Y., Chen Y., Alrtshdi M., Luo W., Zhang J., Qin J., Tang Y. (2016) Monitoring and quantification of the complex bioaccumulation process of mercury (II) in algae by a novel aggregation-induced emission fluorogen. *Royal Society of Chemistry Advances*, vol. 6, pp. 100318-100325.
- Jiang Y., He T., Chen Y., Ruan Y., Zhou Y., Tang B., Qin J., Tang Y. (2017) Quantitative evaluation and in vivo visualization of mercury ion bioaccumulation in rotifers by novel aggregation induced emission fluorogen nanoparticles, *Environmental Science: Nano*, vol. 4, pp. 2186-2192.

- Kasper D., Palermo E. F. A., Dias A. C. M. I., Ferreira G. L., Leitao R. P., Branco C. W. C. and Malm O. (2009) Mercury bioaccumulation in fish of commercial importance from different trophic categories in an Amazon floodplain lake. *Neotropical Ichthyology*, vol. 7, no. 4, pp. 751-758.
- Kelly B. C., Ikonomou M. G., Blair J. D., Morin A. E., Gobas F. A. P. C. (2007) Food web-specific biomagnification of persistent organic pollutants, *Science*, vol. 317, no. 5835, pp. 236-239.
- Lakowicz J. R. (2006) Instrumentation for Fluorescence Spectroscopy. *Principle of Fluorescence Spectroscopy*, Baltimore Maryland, USA.
- Lin H., Wang X., Bi S., Sun C., Yang L. and Liu J (2004) Progress of ICP-MS, NAA and XRF for Al and Al species analysis in Environmental and biological samples, *Journal of Analytical Science*, vol. 20, no. 6, pp. 652-656.
- Liu K. (2005) Review of atomic spectroscopy, *Spectroscopy and Spectral Analysis*, vol. 25, no. 1, pp. 95-103.
- Mei J., Leung N. L. C., Kwok R. T. K., Lam J. W. Y., Tang B., (2015) Aggregation-Induced Emission: together we shine, united we soar! *Chemical Reviews*, vol. 115, pp. 11718-11940.
- Olenick L. (2013) The cautionary tale of DDT – biomagnification, bioaccumulation, and research motivation, Sustainable Nano, <http://sustainable-nano.com/2013/12/17/the-cautionary-tale-of-ddt-biomagnification-bioaccumulation-and-research-motivation>.
- Ruan Z., Li C., Li J., Qin, J., Li Z. (2015) A relay strategy for the mercury(II) chemodosimeter with ultrasensitivity as test strips. *Scientific Reports*, vol. 5, doi: 10.1038/srep15987

- Shukor M. Y., Baharom N. A., Masdor N. A., Abdullah M. P. A., Shamaan N. A., Jamal J. A., Syed M. A. (2009) The development of an inhibitive determination method for zinc using a serine protease. *Journal of Environmental Biology*, vol. 30, no. 1, pp. 17-22.
- Sun B., Zhao L., Ren T., Zhong R. (2012) Progress on detection methods of heavy metals in water environment. *Environmental Science & Technology*, vol. 34, no. 7, pp. 157-162.
- Sun D., Wang X., Hong B. (1999) Sample preparation technique for atomic spectrometric analysis. *Analytical Instrument*, vol. 2, pp. 53-57.
- Tsui M. T. K., Wang W. (2004) Uptake and elimination routes of inorganic mercury and methylmercury in daphnia magna, *Environmental Science and Technology*, vol. 38, no. 3, pp. 808-816.
- Wang E., Zhao E., Hong Y., Lam J. W. Y., Tang B. (2014) A highly selective AIE fluorogen for lipid droplet imaging in live cells and green algae. *Royal Society of Chemistry*, vol. 2, pp. 2013-2019.
- Wei C. (1999), Observation of internal texture of live water flea, *Journal of Wuhan Institute of Education*, vol.18, no.3.
- Xue Y. (2017) Atomic Spectroscopy. *Science Online* , viewed 14 June 2017, <http://highscope.ch.ntu.edu.tw/wordpress/?p=58325>.
- Zhang S., Qin A., Sun J. and Tang B. (2011) Mechanism study of aggregation-induced emission, *Progress in Chemistry*, vol. 23, no. 4, pp. 623-635.
- Zhu Z., Su Y., Li J., Li D., Zhang J., Song S., Zhao Y., Li G., Fan C. (2009) Highly sensitive electrochemical sensor for mercury (II) ions by using a mercury-specific oligonucleotide probe and gold nanoparticle-based amplification. *Analytical Chemistry*, vol. 81, no. 18, pp. 7660-7666.

